Characterisation of Glycine Receptor α2 subunit Interactions with Gephyrin

Aida Muñoz Blázquez

FINAL DEGREE PROJECT

Bachelor's degree in Biotechnology

Academic tutor: Ricardo Román Cordero Otero. Department of Biochemistry and Biotechnology, Universitat Rovira i Virgili, ricardo.cordero@urv.cat

In cooperation with: Rudolf-Virchow-Zentrum (RVZ) – Center for Integrative and Translational Bioimaging, Julius Maximilians Universität Würzburg

Supervisor: Dr. Hans Michael Maric. Group leader. Rudolf-Virchow-Zentrum – Center for Integrative and Translational Bioimaging, Hans.Maric@virchow.uni-wuerzburg.de

June 2022

Jo, Aida Muñoz Blázquez, amb DNI 39933224A, sóc coneixedora de la guia de prevenció del plagi a la URV *Prevenció, detecció i tractament del plagi en la docència: guia per a estudiants* (aprovada el juliol 2017) i afirmo que aquest TFG no constitueix cap de les conductes considerades com a plagi per la URV.

Tarragona, 3 de juny de 2022

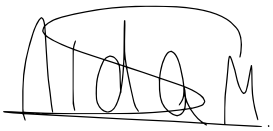

TABLE OF CONTENTS

LIST OF ABBREVIATIONS

DMSO	Dimethyl sulfoxide	PBS	Phosphate-buffered saline
FL-Geph	Full-length gephyrin	PEG	Polyethylene glycol
Fmoc	9-Fluorenylmethyloxycarbony	RSD	Relative Standard Deviation
FPS	Full positional scan	SPPS	Solid-phase Peptide Synthesis
GlyR	Glycine receptor	TFA	Trifluoroacetic acid
$GABA_AR$	γ-Aminobutyric acid type A receptor	TFMSA	Trifluoromethanesulfonic acid
GephE	Gephyrin E domain	TIPS	Triisopropylsilane
HRP	Horseradish-peroxidase	TM	Transmembrane
MP	Milk powder	WT	Wild-type
O/N	Overnight		

CENTER DETAILS

This project has been carried out at the Maric group from the Rudolf-Virchow-Zentrum–Center for Integrative and Translational Bioimaging, Würzburg, Germany, under the supervision of Dr. Hans Michael Maric and Clemens Schulte. The Rudolf-Virchow-Zentrum is a key element of biomedical research at the Julius Maximilians University of Würzburg. AG Maric produces and evaluates chemical libraries on femto molar scale microarrays, thanks to the combination of synthetic chemistry, biology and automated systems. Their ultimate goal is to identify and develop new molecular tools and therapeutic drugs, such as protein inhibitors, *in vitro* evolution approaches and fluorescent probes for super-resolution microscopy. The aim of this project is to characterise the interactions between the α2 subunit of glycine receptor with gephyrin. The work presented here compares results to those from previous experiments conducted in the Maric Lab that are part of former students' thesis and have been unpublished.

SUMMARY

Protein-protein interactions at the postsynaptic membrane mediate inhibitory synaptic transmission. Gephyrin clusters glycine receptors (GlyRs) and γ-aminobutyric acid type A receptors ($GABA_ARs$) at the postsynaptic membrane. So far, gephyrin interactions with GlyR ß and $GABA_ARs$ α subunits have been investigated, but interactions with GlyR α subunits have been overlooked. Here, we explore the interactions of GlyR α2 subunit with gephyrin, expecting an autonomous and specific binding. Protein-peptide interactions can be evaluated at amino acid resolution by binding and neutralisation assays on peptide microarrays containing different types of peptide libraries. As main results, the use of GlyR α2-derived peptides for competition points towards a longer sequence, gephyrin binding hierarchy shows GlyR α2 as the strongest binder among α subunits, and profiling of gephyrin-GlyR α2 interactions revealed a possibly partially overlapping binding site with GlyR ß and $GABA_ARs$ α subunits. Single point gephyrin mutants revealed specifically GlyR α2 binding.

Key words: gephyrin, glycine receptor, protein-protein interactions, binding, peptide microarray.

1. INTRODUCTION

1.1. Glycine Receptors

Glycine Receptors (GlyRs) are the main inhibitory receptor in the central nervous system. They are localized at the postsynaptic membrane of motor neurons. Glycinergic synapse predominates in adult brainstem and spinal cord. GlyRs are ligand-gated ion channels, known for mediating fast neurotransmission. They comprise chloride-selective pores that open upon glycine binding. Chloride influx leads to hyperpolarization of the membrane of motor neurons. Accordingly, functional GlyRs perform a feedback control loop to ultimately dampen excitation and balance motor neuron firing (Langlhofer et al., 2016; Schaefer et al., 2012).

There are four GlyR α subunits (α1-α4) and one GlyR ß subunit known. They assembly as either heteropentamers, usually in stoichiometry 2α:3ß or 3α:2ß, or homopentamers, only composed of α subunits. Recently, a stoichiometry of heteromeric receptors was described as 4α:1β (Yu et al., 2021; Zhu et al., 2021). GlyR α2 subunit forms homopentameric receptors in the embryonic stage starting at day E15. The switch from the GlyR neonatal to the GlyR adult isoform is completed by postnatal day 20. The adult isoform is composed of α1ß heteromers in the spinal cord. However, GlyR α2 subunit expression persists in adulthood in retina, cerebellum and autidory brainstem (Schaefer et al., 2012). All subunits may be subject to alternative splicing, conferring functional diversity to the receptor (Langlhofer et al., 2016).

GlyR disfunction has been associated with hyperekplexia, a rare neuromotor disorder also known as startle disease. Single point mutations in the *Glra1* and *Glrb* genes, respectively encoding the GlyR α1 and GlyR ß subunits, resulted in pathological phenotypes in mouse models. For example, the *oscillator* mouse mutant presents a loss-of-function mutation, neuromotor symptoms and a lethal phenotype (Schaefer et al., 2012). It also showed impairment in the respiratory rhythm. Besides, glycinergic neurotransmission is a key mechanism of pain sensitisation. GlyR α1 and α3 subunits are involved in chronic inflammatory pain and spinal glycinergic disinhibition *via* post-translational modifications (San Martín et al., 2022).

The GlyR is a Cys-loop receptor. It has four transmembrane (TM) domains. The ion channel pore is located in the TM2. The large TM3-4 intracellular loop is highly variable regarding length and sequence. Its structure has not been resolved yet due to its presumably disordered nature. Further post-translational modifications modulate the ion channel properties. GlyRs clustering and localization at the postsynaptic membrane depends on the intracellular domain interaction with other proteins. The large TM3-4 loop interaction with gephyrin allows the receptor to be clustered at the postsynaptic membrane (Langlhofer et al., 2016).

1.2. Gephyrin

Gephyrin is the main scaffolding protein of the inhibitory postsynapse. Gephyrin comprises three domains: the functional G- and E-domains, linked by the C-domain. The former domains are similar to the bacterial MogA and MoeA proteins, involved in molybdenum cofactor synthesis (Groeneweg et al., 2018).

Gephyrin mRNA has a complex intron-exon structure and is subject to alternative splicing in a cell- and tissue-specific way. Post-translational modifications, like phosphorylations on its C-domain, have been widely reported. Interactions with other synaptic proteins like collybistin and neuroligins play a role in gephyrin clustering. Therefore, splice variants, post-translational modifications and interaction with other proteins regulate gephyrin's synaptic and non-synaptic functions. Gephyrin's structure, localization, density and scaffolding properties might be affected, contributing to the plasticity of inhibitory synapses (Groeneweg et al., 2018; Alvarez, 2017).

Besides, gephyrin interacts with the actin cytoskeleton and motor proteins. Motor protein complexes of GlyR and dynein are coupled by gephyrin scaffold. GlyRs and gephyrin undergo retrograde axonal cotransport (Maas et al., 2006).

1.3. Glycine Receptor and Gephyrin

Gephyrin clusters GlyRs and γ-aminobutyric acid type A receptors ($GABA_ARs$) at postsynaptic sites. $GABA_ARs$ are pentameric ionotropic receptors. The binding affinity of gephyrin to GlyR ß subunit is 25-fold higher than to $GABA_AR$ α3 subunit (Maric et al., 2014)

The importance of gephyrin for GlyR clustering at the postsynaptic membrane was clear-cut demonstrated. First, the silencing of gephyrin expression with antisense oligonucleotides prevents GlyR from clustering at the postsynaptic membrane (Kirsch et al., 1993). Moreover, gephyrin knock-out mice also prevented GlyR clustering (Kneussel et al., 1999).

For binding to happen, gephyrin E domains (GephE) dimerize. Specifically, the binding pocket is located between GephE subdomain IV and partially subdomain III (Maric et al., 2011). The intracellular loop of GlyR ß subunit binds gephyrin in a 2:1 gephyrin-to-ß-subunit ratio. This estimated proportion suits the hexagonal lattice structure model of oligomerization of gephyrin (Tyagarajan et al., 2014).

Protein-protein interactions interface can be minimized to a cluster of hotspot residues. Gephyrin most studied binding peptides have mainly hydrophobic residues extremely conserved, especially between GlyR ß and $GABA_AR$ α3 subunits. The sequence of GlyR ß subunit mainly interacting with gephyrin had been determined to be ^{398}FSIVGSLPRDFEL^{410}. The N-terminal gephyrin-binding motif is conserved in the GlyR ß and $GABA_AR$ α3 subunits, being FSIVG and FNIVG, respectively. GlyR ß subunit and $GABA_ARs$ compete for a mutually exclusive overlapping gephyrin-binding site, which suggest that their clustering and transport to the synapse is interdependent (Maric et al., 2017).

A gephyrin consensus peptide-binding motif has been established based on peptide array screen and alignment of fine mapped gephyrin binding sites (Table 1).

Table 1. Gephyrin consensus peptide-binding motif. Hydrophobic residues (orange) are highly conserved. Adapted from Maric et al. (2017).

	Binding Motif										
Position	0	1	2	3	4	5	6	7	8	9	10
Consensus	Ω	ζ	Ψ	Ψ	G	ζ	x	P/Y	f_c		
GlyR ß	^{398}F	S	I	V	G	S	L	P	R	D	F
GABA$_A$R α1	^{340}Y	A	P	T	A	T	S	Y	T	P	I
GABA$_A$R α2	^{338}A	Y	A	V	A	V	A	N	Y	A	P
GABA$_A$R α3	^{368}F	N	I	V	G	T	T	Y	P	I	N
GABA$_A$R α5	^{379}A	F	T	T	G	D	M	S	H	P	P

Ω: aromatic, ζ: hydrophilic, Ψ: large aliphatic, x: not conserved,

f_c: flanking ligand core at the C-terminus

Figure 1 shows a close-up view of the GlyR ß-derived peptide binding to GephE, as well as interactions between their residues.

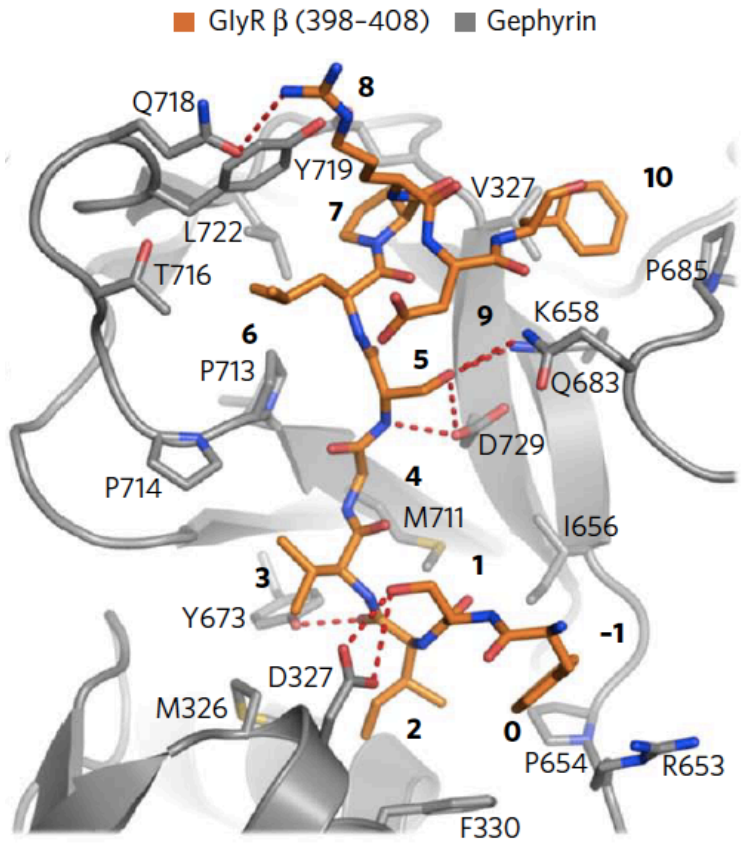

Figure 1. Close-up view of the GlyR ß-derived peptide binding to GephE. X-ray crystal structure of GlyR ß residues 398-408 is represented by the orange stick model (Maric et al., 2017).

Due to the involvement of GlyRs and $GABA_ARs$ with neurological pathologies, they are acknowledged drug targets. Novel approaches focus on the intracellular receptor-gephyrin interaction. Gephyrin super-binding peptides exert their pharmacological action through high-affinity binding to the receptor-binding site. Further developed gephyrin super-binding peptides could modulate inhibitory neurotransmission by the modulation of receptor clustering (Maric et al., 2017). Maric et al. (2015) demonstrated that dimeric peptides bind gephyrin with picomolar affinity, being potent gephyrin binders by targeting two GephE domains simultaneously. Optimization was conducted by sequence fine-tuning and the use of a polyethylene glycol (PEG) linker.

Whereas GlyR ß subunit binding to gephyrin has been broadly studied, interactions between gephyrin and GlyR α subunits have not been well characterised yet. Previous experiments in the Maric lab showed GlyR α2 subunit as the third stongest gephyrin binder after GlyR ß and $GABA_AR$ α3 subunits. Considering GlyR α subunits within the heteropentameric receptor and the multimeric nature of gephyrin, GlyR α subunits are likely to contribute to GlyR binding to gephyrin. Moreover, despite that embryonic GlyRs are homomeric receptors only formed by GlyR α2 subunits, the implication of GlyR α2 in the embryonic glycinergic synapse through binding to gephyrin has been unnoticed. Thus, binding of GlyR α2 subunit to gephyrin has been underestimated and not studied.

The aim of this project is to explore the interaction of GlyR α2 subunit with gephyrin. Previous experiments' reproducibility in the Maric lab will be tested. GlyR α2 subunit binding to gephyrin will be attempted to challenge by competition with short GlyR α2 dimeric peptides.

2. HYPOTHESIS

Glycine Receptor α2 subunit is able to bind autonomously and specifically to gephyrin.

3. MATERIALS AND METHODS

3.1. Materials

Devices used are listed in table 2.

Table 2. List of devices.

Device	Source	Product name
Balances	A&D Company Idt.	FZ-300i
Centrifuge rotors	Thermo Scientific	M-20
Centrifuges	Labnet	Prism R
Imaging system	Azure	C400
Microarray contact printer	Intravis	SlideSpotter
Multichannel pippete	Brand	Transferpette S-12
Orbital shaker	Scientific Industries	Mini-100 Orbital-Genie
Peptide synthesizer	Intravis	MultiPrep Rsi
pH-meter	VWR	pHenomenal pH 1100L
Pipette	Rainin Rainin Rainin Eppendorf	Pipet-Lite LTS Pipette L-1000XLS+ Pipet-Lite LTS Pipette L-200XLS+ Pipet-Lite LTS Pipette L-20XLS+ Research ® plus 0.1-2.5 µL
Pippetteboy	Brand	Accu-jet pro
Stepper pippete	Eppendorf	Multipette M4
Thermoshaker	Eppendorf	Eppendorf Thermomixer comfort
Vortex	Scientific Industries	Vortex-Genie 2

Consumables used are listed in table 3.

Table 3. List of consumables.

Consumable	Source	Product name
Conical tubes	Sarstedt	15, 50 mL
Gloves	VWR	NITRILE Light
Pipette tips	Biozym Eppendorf	SurPhob 20, 200, 1000 µL epT.I.P.I.S® reload 2 µL
Reaction tubes	Sarstedt	1.5, 2 mL
Serological pippete	Sarstedt	5, 10, 25 mL
Well plates	Eppendorf Intravis	Deepwell Plate 96/1000 µL 384 well plate

Resources used are listed in table 4.

Table 4. List of reagents and resources.

Resource	Source	Identifier
Antibodies and detection reagents:		
Monoclonal mouse anti-gephyrin (3B11)	Synaptic Systems	14711
Goat anti-mouse (HRP conjugate)	Invitrogen	31430
SuperSignal West Femto Maximum Sensitivity Substrate	Invitrogen Thermo Scientific	84545 34095
Cellulose Paper:		
Whatman Grade 50	GE Healthcare	1450-916
Proteins:		
GephE (residues 318-736)	(Schrader et al., 2004)	N/A
Full-length gephyrin (FL-Geph)		N/A
Native gephyrin from mouse brain lysate	RVZ Würzburg	N/A
Slides:		
White coated slides (CelluSpot blank slides)	Intravis	54.112

Chemicals including buffer ingredients, solvents and reagents were purchased from Iris, Sigma-Aldrich, Carl Roth or VWR.

All amino acids and derivatives used in solid phase peptide synthesis (SPPS) were protected with 9-Fluorenylmethyloxycarbony (Fmoc) group at their N-terminus and their respective side chain, and are listed in Table 5.

Table 5. . List of aminoacids and derivatives used in SPPS.

Derivative	Code	Chemical name (abbr.)	Source	Identifier
PEG-linker	O	Fmoc-O2Oc-OH	Iris	FAA1435
L-Alanine	A	Fmoc-L-Ala-OH·H2O	Iris	FSP1005
β-Alanine	B	Fmoc-beta-Ala-OH	Iris	FAA1300
L-Cysteine	C	Fmoc-L-Cys(Trt)-OH	Iris	FSC1040
L-Aspartic acid	D	Fmoc-L-Asp(tBu)-OH	Iris	FSP1020
L-Glutamic acid	E	Fmoc-L-Glu(tBu)-OH·H2O	Iris	FSP1045
L-Phenylalanine	F	Fmoc-L-Phe-OH	Iris	FSA1175
Glycine	G	Fmoc-Gly-OH	Iris	FSC1050
Glycine	G	Boc-Gly-OH	Novabiochem	853000
L-Histidine	H	Fmoc-L-His(Trt)-OH	Iris	FSP1090
L-Isoleucine	I	Fmoc-L-Ile-OH	Iris	FSC1110
L-Lysine	K	Fmoc-L-Lys(Boc)-OH	Iris	FSC1125
L-Lysine	K	Fmoc-L-Lys(Fmoc)-OH	Iris	FAA1391
L-Leucine	L	Fmoc-L-Leu-OH	Iris	FSP1120
L-Methionine	M	Fmoc-L-Met-OH	Iris	FAA1150
L-Asparagine	N	Fmoc-L-Asn(Trt)-OH	Iris	FSC1015
L-Proline	P	Fmoc-L-Pro-OH·H2O	Iris	FAA1185
L-Glutamine	Q	Fmoc-L-Gln(Trt)-OH	Iris	FSC1043
L-Arginine	R	Fmoc-L-Arg(Pbf)-OH	Iris	FSC1010
L-Serine	S	Fmoc-L-Ser(tBu)-OH	Iris	FSC1190
L-Threonine	T	Fmoc-L-Thr(tBu)-OH	Iris	FSP1210
L-Valine	V	Fmoc-L-Val-OH	Iris	FSC1245
L-Tryptophan	W	Fmoc-L-Tryptophan-(Boc)	Carl Roth	9668
L-Tyrosine	Y	Fmoc-L-Tyr(tBu)-OH	Iris	FSP1230

Software used to perform experiments, analyze data and design figures within this work is listed in Table 6.

Table 6. List of software used.

Software	Reference
Fiji (ImageJ)	https://fiji.sc/
Laura	Intravis
Microsoft Office	https://www.microsoft.com/de-de/microsoft-365
GraphPad Prism 9	https://www.graphpad.com/scientific-software/prism/

3.2. Methods

3.2.1. Solid-Phase Peptide Synthesis

Solid-Phase Peptide Synthesis (SPPS) was performed by my supervisor from RVZ Würzburg. Firstly, SPPS is performed on 2-Chlorotrityl Chloride Resin. Steps are loading the first amino acid, removing the Fmoc protecting group, coupling the subsequent amino acids, capping the truncated amino acid chains after coupling, and cleaving the finished peptide from the resin.Then, automated SPPS is carried out on cellulose.

3.2.2. Work-Up of Cellulose-Peptide Conjugates

Side Chain Deprotection

The acid-labile amino acid side chain protection groups are removed using 150 µL of a deprotection mix. The deprotection mix contains trifluoroacetic acid (TFA), triisopropylsilane (TIPS), H_2O and dichloromethane, in a respective ratio by volume of 90:3:5:2. The 96 deep-well plates are shaken for 2 h at 1000 rpm and room temperature. The supernatant is discarded.

Cellulose Conjugate Dissolution

Cellulose conjugates are dissolved using 200 µL of a disintegration mix. The disintegration mix contains TFA, trifluoromethanesulfonic acid (TFMSA), TIPS and H_2O, in a respective ratio by volume of 88.5:4:3:4.5. The plates are incubated for 30 min at room temperature. Plates are shaken at 500 rpm overnight (O/N) until fully dissolved.

Cellulose Conjugate Precipitation

Cellulose conjugates are purified using 500 µL diethyl ether. The cellulose conjugates are left to precipitate for at least 2h at -20 °C. Afterwards, the plates are centrifuged for 5 min at 1500 rpm and 4 °C. The supernatant is discarded. The process is repeated two more times. When the cellulose pellet is dry, 250 µL dimethyl sulfoxide (DMSO) is added and pellets are dissolved by O/N shaking. The plates with the dissolved cellulose-peptide conjugates can be stored at -80 °C.

3.2.3. Transfer of Cellulose Peptide Conjugates into Microarray Format

The peptides dissolved in DMSO are transferred from a 96-deep well plate into a 384-well plate. Peptides are mixed in a ratio of 2:1 with saline-sodium citrate buffer (150 mM NaCl, 15 mM trisodium citrate, pH 7.0). Using a liquid handling robot (SlideSpotter; Intavis) the peptides are spotted on nitrocellulose coated slides (Intavis) in a 2 x 16 x 24 format. There is an internal replication of the library per slide. The dispensed volume is 0.05 µL per spot. After spotting, slides can be left to dry and stored at 4ºC.

3.2.4. Mouse Brain Lysate

Freezed mouse brains were kindly provided by associates from RVZ Würzburg. Lysate is obtained by manually smashing and addition of 500 µL HEPES buffer while kept in ice. Lysates are sonicated, centrifugated for 30 min at 4ºC at maximum speed, and pellet is discarded. Finally, aliquotes from a mixture of all lysates are flash-freezed in liquid nitrogen and stored at -80ºC.

3.2.5. Peptide Microarray Binding Assay

Unspecific binding on the microarray slides is blocked with 3 mL of 5 % milk powder (MP) in 1x phosphate-buffered saline (PBS); 137 mM NaCl, 2.7 mM KCl, 10 mM Na_2HPO_4, 1.8 mM KH_2PO_4, pH 7.4) for 1 h at ~60 rpm at room temperature on an orbital shaker. Blocking solution is removed. Next, 2.5 mL of the protein of interest (recombinant GephE, FL-geph or native gephyrin in mouse brain lysate) solubilised in 5 % MP in PBS is applied for 15 min. The slides are washed three times for 3 min with ~3 mL PBS. To mark the bound protein for

later detection, the slides are incubated with 2.5 mL of an anti-gephyrin-antibody (3B11; Synaptic Systems) at a 5000-fold dilution in 5 % MP in PBS. A second washing step is conducted. Slides are incubated with secondary antibody a 5000-fold dilution in 5 % MP in 2.5 mL PBS. The secondary antibody is goat anti-mouse conjugated with horseradish-peroxidase (HRP; Invitrogen). A third washing is conducted. Peptide binding is detected *via* enhanced chemiluminiscence using a c400 imaging system (Azure), by adding 200 µL per slide of SuperSignal West Femto Maximum Sensitive Substrate (Thermo Scientific) at lowest chemosensitivity. The resulting images are analysed with the image editing software Fiji (ImageJ) and its plugin “Microarray Profile”. Mean signal of the background is measured and subtracted for every side of the slide. The grid of the plugin is applied to measure the intensity values of the spots.

3.2.6. Peptide Microarray Neutralisation Assay

Binding assays results can be verified by on-chip peptide neutralisation. The neutralisation assay protocol is similar to the microarray binding assay, except for a preincubation step parallel to the blocking. The protein of interest and the competitor peptide are mixed in a total volume of 150 µL with PBS. The vial is shaken for 30 min at 300 rpm at room temperature. The protein-peptide solution is diluted to a volume of 2.5 mL and applied to the microarray slide.

4. RESULTS

The peptide libraries used in this project are summarized in Table 7.

Table 7. Libraries used in this project. Complete libraries can be found in Suppl. Tables 1, 2 and 3.

Type	Design	Sequence
Overlapping Library	20 amino acids 17 overlap 3 off-set	TM3-4 loop of $GABA_AR$ α, $GABA_AR$ γ1, and GlyR subunits, except GlyR ß and $GABA_AR$ α3
Truncation Library	20 amino acids Truncation at N- and C-terminus	GlyR α1: ^{364}EGGEGRFNFSAYGMGPACLQ^{384} GlyR α2: ^{364}VTRESRFNFSGYGMGHCLQM^{383} GlyR α3: ^{366}FYRFSDTDDEVRESRFSFTA^{385} GlyR α4: ^{364}IIRESRFYFRGYGLGHCLQA^{383}
Full Positional Scan (FPS) Library	7 amino acids 133 Point-mutated variants 7 wild-type sequences	GlyR α2: ^{370}FNFSGYG^{376}

4.1. Use of Glycine Receptor-Derived Peptides for Competition

Initially, the interaction of gephyrin with sequences of the GlyR α subunits was evaluated using a truncation library. Binding of recombinant GephE was compared to native gephyrin from mouse brain lysate (Suppl. Figure 1). Peptides used in the following competition assays are specified in Table 8.

Table 8. GlyR-derived competitor peptides. O=PEG linker.

Name	Subunit	Sequence	Type
B11C	GlyR ß	(^{398}FSIVGSLPRDF^{408}C)	Wild-type
A2D5	GlyR α2	(^{372}FSGYG^{376}OO)$_2$K	Wild-type
A2D7	GlyR α2	(^{370}FNFSGYG^{376}OO)$_2$K	Wild-type
DB1D	GlyR α2	(^{366}RESRFNFSGYGMGHC^{376}O)$_2$K	Wild-type
DB3D	GlyR α2	(^{366}RESRANFSGYGMGHC^{376}O)$_2$K	Ala-mutant

Aiming to recapitulate the high-affinity binding of GlyR ß subunit to gephyrin, a competition assay with a GlyR ß subunit-derived peptide was carried out. The peptide in solution competes with the peptides printed on the microarray for gephyrin binding. Presuming an overlapping binding site, if the competitor peptide interacts with gephyrin with higher affinity, no binding between gephyrin and the on-chip peptide sequence would take place. The competitor peptide B11C includes the gephyrin binding motif formerly described, and was synthetised and purified by Dr. Hans Michael Maric, RVZ Würzburg. The competition assay was conducted using GephE at 200 nM and B11C at different concentrations.

A truncation library with GlyR α subunits' gephyrin-binding sequences was used. Truncation libraries verify the binding hotspot identified in the overlapping library screening. The design of this library involved shortening 20-mer peptides by one amino amid at the time both at N- and C-terminus, until reaching a length of 6 amino acids.

From the μSPOT readouts (Suppl. Fig 2), total binding intensities of the GlyR α2 spots were represented in Figure 1. The accumulative binding intensities were normalised to the no-peptide condition. Increasing concentration of B11C correlates with a decline of GephE-GlyR α2 binding. These results are consistent with previous experiments in the Maric group.

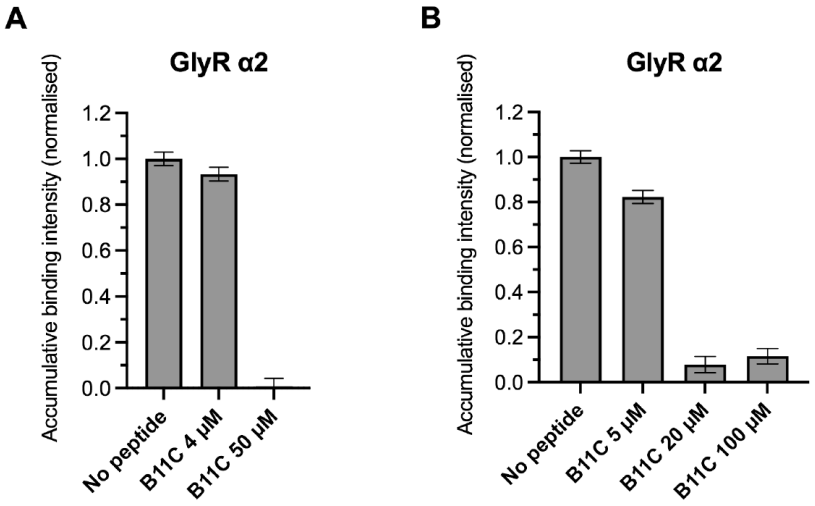

Figure 2. Competition assay using B11C as competitor peptide and GephE at 200nM. Accumulative binding intensity of the GlyR α2 spots is graphed for every neutralisation condition. No peptide condition values are normalised to 1. Error bars represent the Relative Standard Deviation (RSD) values. Raw data can be found in Suppl. Fig. 2.

Following the gephyrin-binding peptides design and optimization (Maric et al., 2015), GlyR α2-derived peptides were synthesized based on its gephyrin binding sequence identified in previous studies. Dimeric architecture and the use of PEG linkers were common features.

Former experiments in the Maric lab ("Characterisation of Glycine Receptor α Subunit Interactions with Gephyrin" by David Baumstark) used as competitor a dimeric 15-mer α2-derived peptide. DB1D showed a good competition ability against GlyR α subunits peptides on the array, compared to binding in absence of peptide and to its respective F372A mutant DB3D. DB3D served as a negative control owing to its reduced neutralisation effect as a monomer.

Computational approaches allowed determining shorter versions of the GlyR α2 gephyrin binding sequence. The peptide sequences were either 5 (^{372}FSGYG^{376}, "A2D5") or 7 (^{370}FNFSGYG^{376}, "A2D7") amino acids long. Two PEG linkers are intended to compensate for potential difficulties in the dimeric peptides interaction with gephyrin due to close proximity of the C-terminal amino acids, as well as enhance solubility. Competition assays were performed using a truncation library, GephE at 200 nM and different concentrations of competitor peptides. Figure 2 shows the normalised accumulative binding intensity for GlyR α2 spots after competition assays with A2D5 (Figure 3A), A2D7 at the same conditions (Figure 3B), and A2D7 at higher concentrations (Figure 3C).

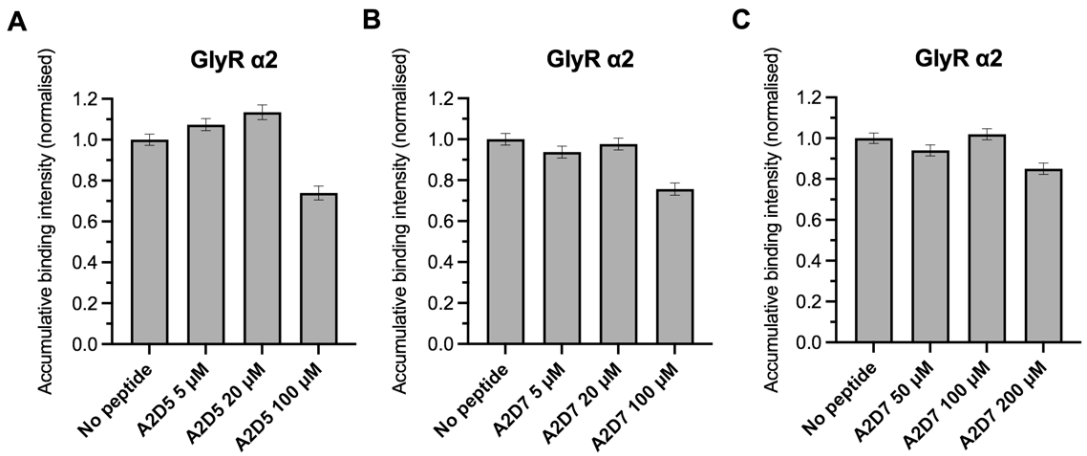

Figure 3. Competition assay using GephE at 200 nM and (A) A2D5 at 5, 20 and 100 µM; (B) A2D7 at 5, 20 and 100 µm; (C) A2D7 at 50, 100, 200 and 400 µM, as competitor peptides. Accumulative binding intensity of the GlyR α2 spots is graphed for every neutralisation condition No peptide condition values are normalised to 1. Error bars represent the RSD values. Raw data can be found in Suppl. Fig. 3.

To test reproducibility of previous studies, DB1D and DB3D were also used in competition assays using a truncation library and GephE at 200 nM. Figure 4 shows the normalised accumulative binding intensity for GlyR α2 spots after competition assays with DB1D and DB3D at 50 and 100 µM each peptide.

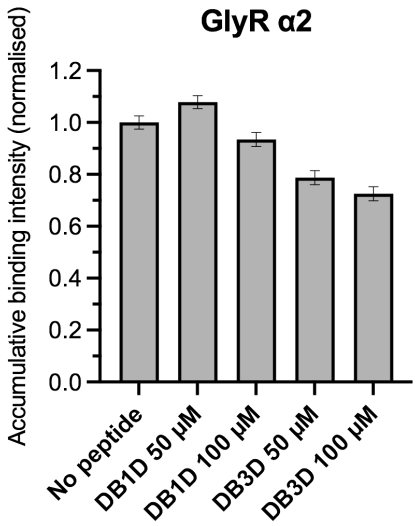

Figure 4. Competition assay using DB1D and DB3D at 50 and 100 µM each as competitor peptide and negative control, respectively, and GephE at 200 nM. Accumulative binding intensity of the GlyR α2 spots is graphed for every neutralisation condition. No peptide condition values are normalised to 1. Error bars represent the RSD values. Raw data can be found in Suppl. Fig. 4.

4.2. Recapitulating Gephyrin-Glycine Receptor α subunits Binding Hierarchy

Binding hierarchy of GlyR α subunits to gephyrin could be recapitulated with the truncation scan results by comparing binding intensities of the four GlyR α subunits normalised to the highest value overall (Figure 5A, Suppl. Figs. 1-4, “No peptide” results). Moreover, specific contributions of single amino acids to the peptide binding affinity binding can be quantified with a truncation library. A drop of the binding intensity between a given peptide and another sequence one amino acid shorter might suggest that particular amino acid as crucial for binding affinity.

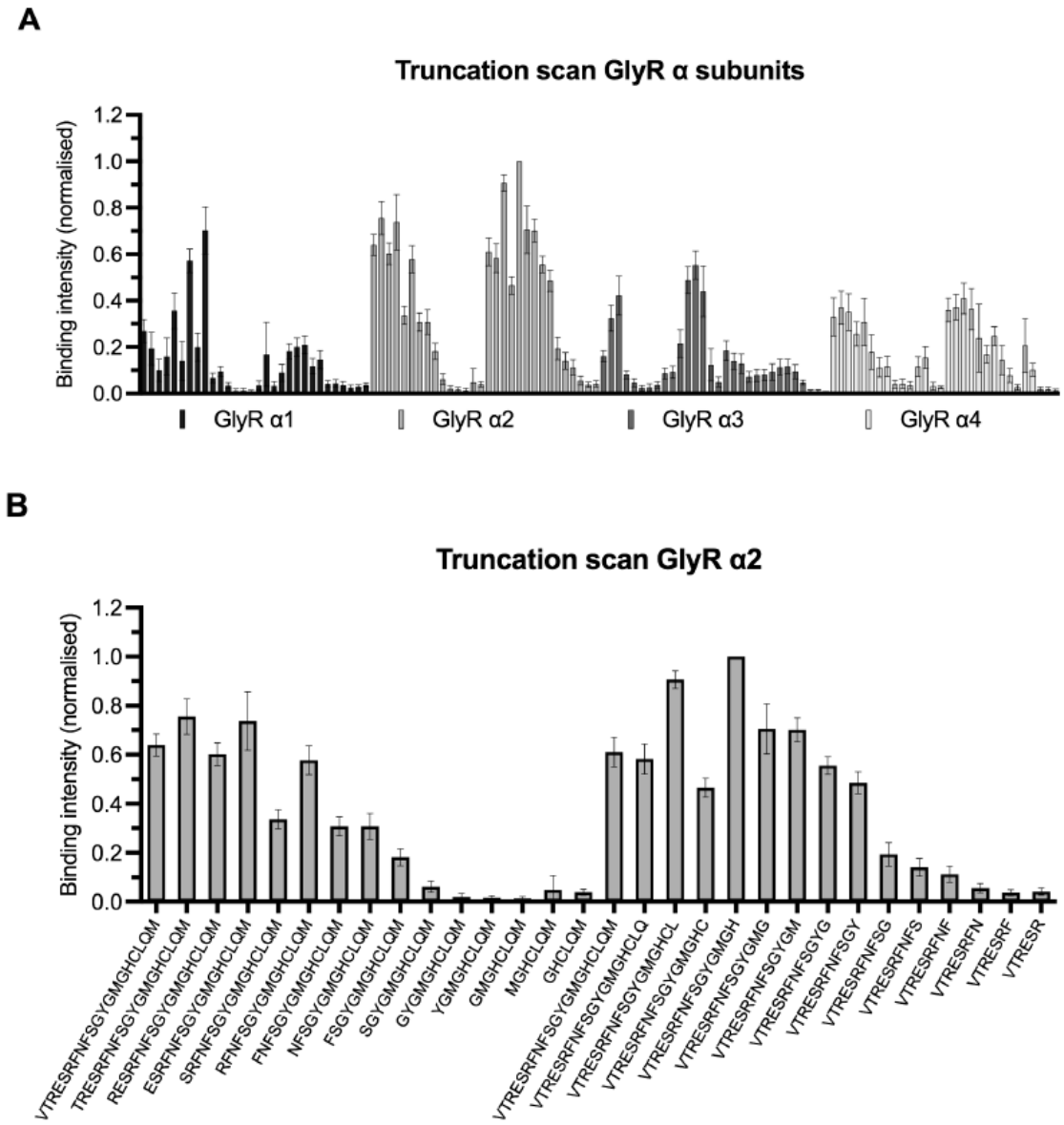

Figure 5. (A) Truncation scan of GlyR α subunits. Binding intensities normalised to highest value overall. (B) Truncation scan of GlyR α2 subunit. Binding intensities normalised to highest value from GlyR α2 subunit spots. Results shown as mean of n=7. Error bars represent the RSD values.

DB1D neutralisation potential was attempted to be again validated in a competition assay using the $GABA_AR$/GlyR overlapping library described in Table 7. In this library, overlapping peptides corresponding to the TM3-4 loop of GlyR α1-4, $GABA_AR$ α1-2 and α4-6, and $GABA_AR$ γ subunits are displayed on the array. The library was pippeted without peptides corresponding to GlyR ß nor $GABA_AR$ α3 subunits. This way, low-affinity gephyrin binders can be detected. Peptides length is 20 amino acids with an offset of 3 amino acids.

Accumulative binding intensity of the GlyR α subunits spots was normalised to their respective no peptide condition (Figure 6).

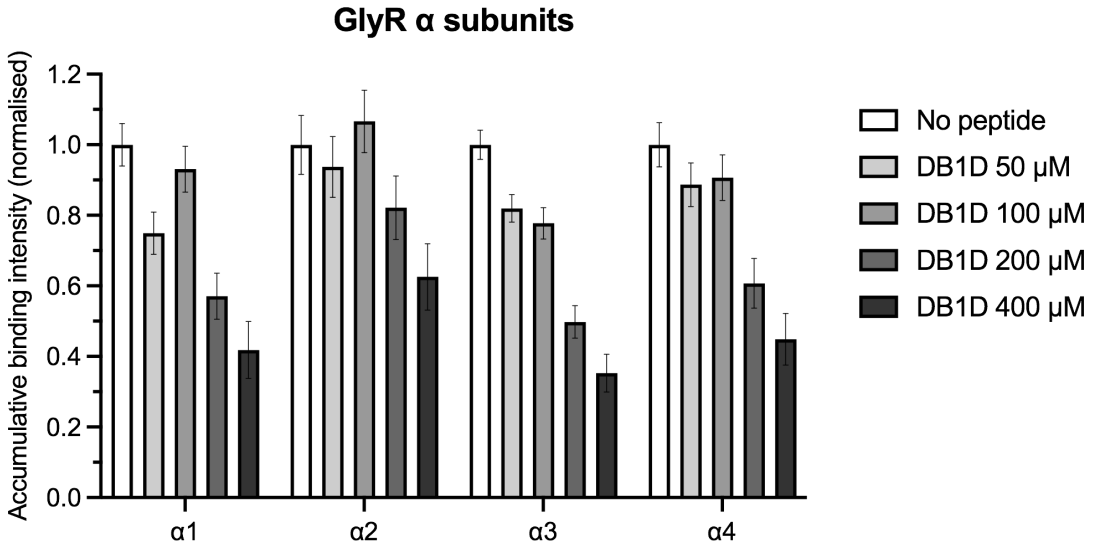

Figure 6. Competition assay using DB1D as competitor peptide and GephE at 200 nM. A $GABA_AR$/GlyR α subunits overlapping library was used. Accumulative binding intensities normalised to no peptide condition for each GlyR α subunit. Error bars represent the RSD values. Raw data can be found in Suppl. Fig. 5.

4.3. Profiling of Glycine Receptor α2 Interaction with Gephyrin

To gain a deeper understanding of the way gephyrin interacts with GlyR α2, binding assays with GephE, full-length gephyrin (FL-Geph) and mouse brain lysate were performed (Figure 7). FL-Geph allowed for assessment of differences in the binding pattern due to structural reasons and the presence of the G- and C-domains. Native gephyrin from mouse brain lysate served for considering additional gephyrin interactors in its native context.

A Full Positional Scan (FPS) library was synthesized based on the sequence ^{370}FNFSGYG^{376} from the GlyR α2 subunit. The seven positions were systematically probed with every 20 proteogenic amino acids, amounting to 133 peptide variants and 7 wild-type sequences. Spots from positions A1-F20 (Suppl. Fig 6) correspond to the sequence ^{370}FNFSGYG^{376}. Spots from positions G1-L20 correspond to the sequence ^{370}FNFSGYG^{376}OO; two PEG linkers at the C-terminus act as spacers between the peptide sequence and the cellulose paper.

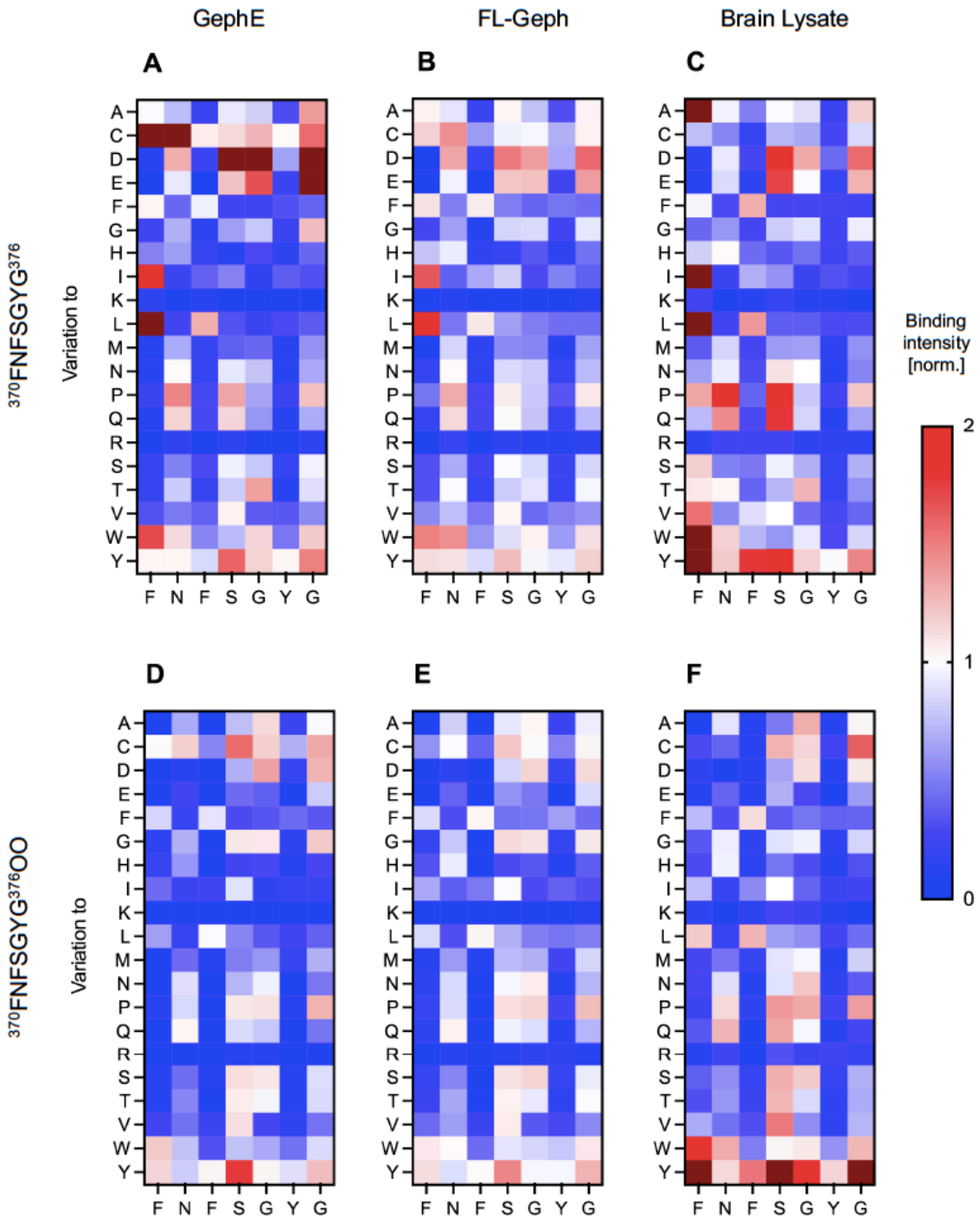

Figure 7. FPS of GlyR α2 gephyrin binding motif. Binding assays were performed using GephE at 200 nM, FL-Geph at 200 nM, and 20 µL of native gephyrin from brain lysate (columns). Library based on raw FNFSGYG sequence (upper row) and FNFSGYGOO sequence (lower row). Binding intensity values are presented as mean of n=3, normalised to the wild-type sequence values (n=7) and displayed as a heatmap. Maroon cells represent values greater than 2. O=PEG linker. Raw data can be found in Suppl. Fig. 6.

The next goal was the evaluation of the binding capabilities of the GlyR α2-derived dimeric peptide A2D7 in solution compared to the same sequence printed in microarray format. For that purpose, a competition assay using A2D7 on a FPS library was carried out (Figure 8A). To validate this assay, a competition assay with the high affinity gephyrin-binding GlyR ß-derived peptide B11C was conducted (Figure 8B).

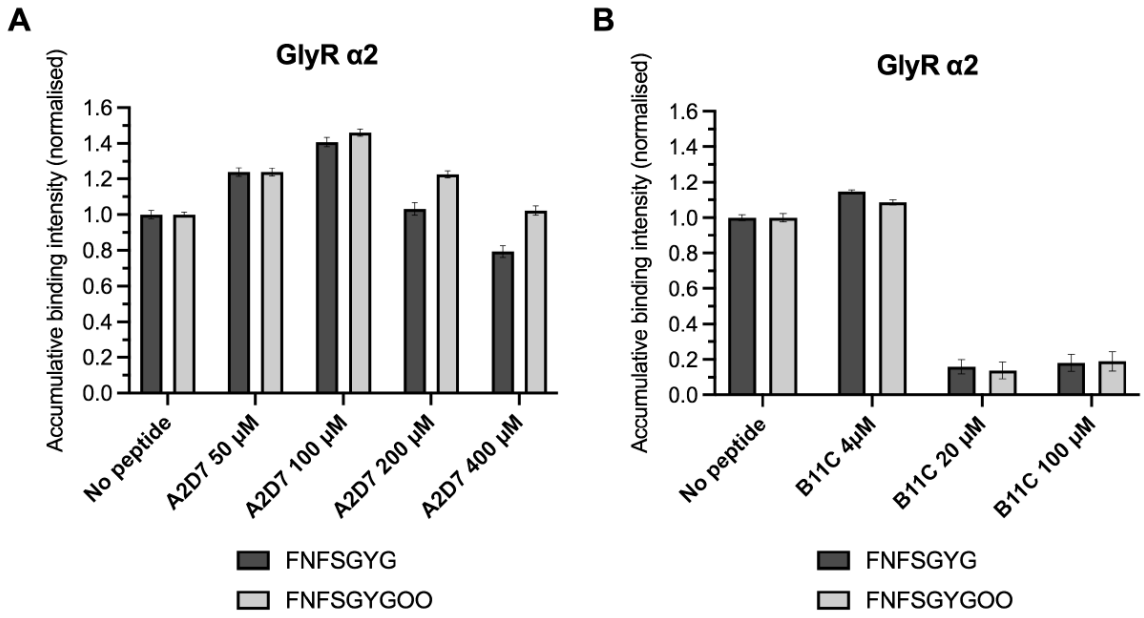

Figure 8. Competition assay using GephE at 200 nM and (A) GlyR α2-derived dimeric peptide A2D7; (B) GlyR ß-derived peptide B11C as competitor peptides. A FPS library was used. Accumulative binding intensties from wild-type sequences are normalised to no peptide condition. . Error bars represent the RSD values. Raw data can be found in Suppl. Fig. 7.

Further experiments with the FPS library included the assessment of GlyR α2 residues ^{370}FNFSGYG^{376} contribution to binding using GephE point mutants F330A and P713E, previously determined as critical for GlyR ß, $GABA_AR$ α1 and $GABA_AR$ α3 subunits binding (Eun et al., 2006; Maric et al., 2011; Maric et al., 2017).

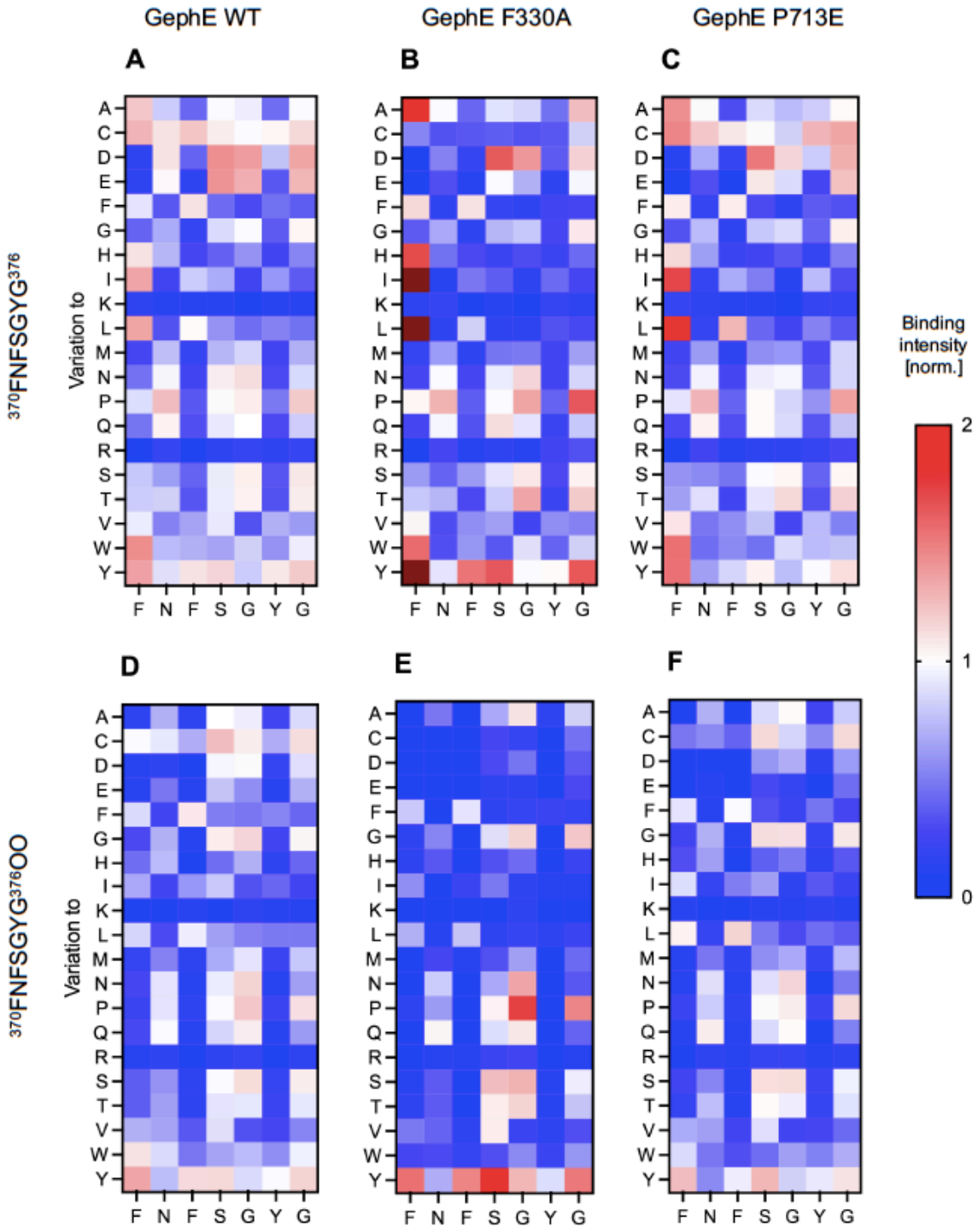

Figure 9. FPS of GlyR α2 gephyrin binding motif. Binding assays were performed using wild-type GephE (GephE WT), GephE mutant F330A and GephE mutant P713E, at 200 nM each (columns). Library based on raw FNFSGYG sequence (upper row) and FNFSGYGOO sequence (lower row). Values are presented as mean of n=3, normalised to the wild-type sequence values (n=7) and displayed as a heatmap. Maroon cells represent values greater than 2. O=PEG linker. Raw data can be found in Suppl. Fig. 8.

The effect of the GephE point mutants on the GlyR α2 subunit hotspot can be broadly assessed by the reduction of the binding intensity of wild-type sequences of the library (Figure 10). Raw values of the wild-type sequences for every condition were normalised to the mean value for wild-type GephE (GephE WT). Statistical analysis one-way ANOVA and multiple comparison was performed.

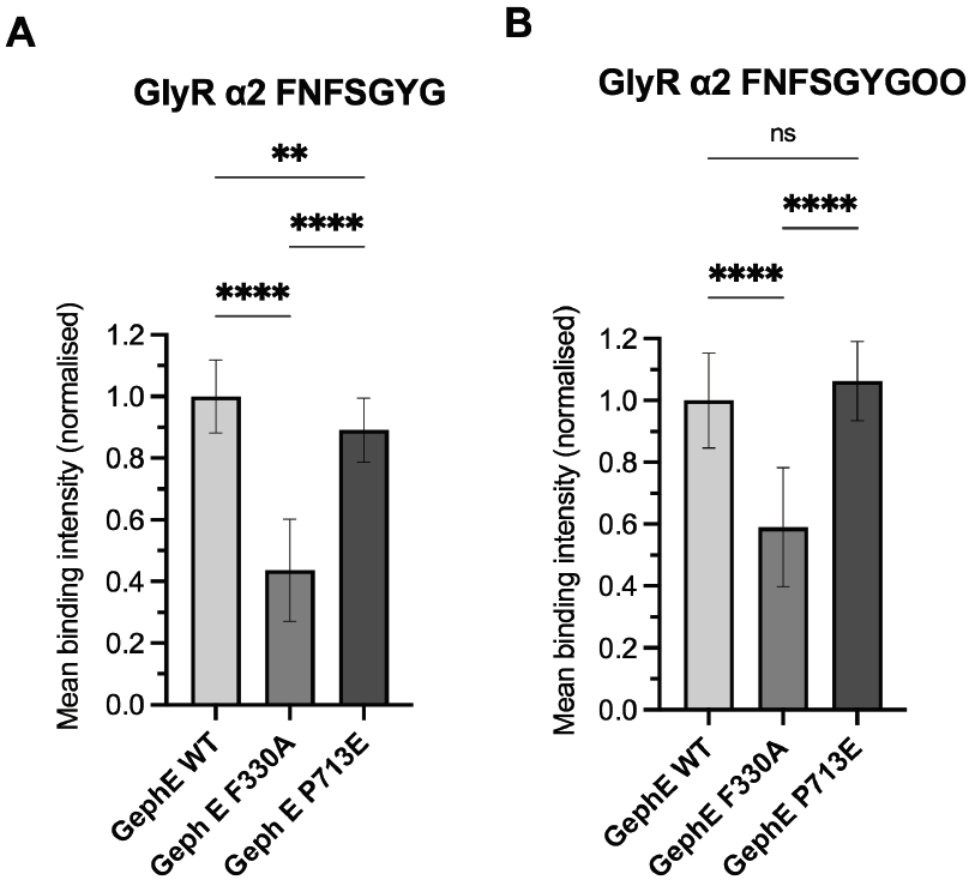

Figure 10. Binding intensity values of wild-type sequences (n=21) normalised to the mean value of GephE wild-type. Normalised mean values for (A) FNFSGYG spots and (B) FNFSGYGOO spots are represented. Binding assays performed using the GlyR α2 FPS library and GephE WT, GephE mutant F330A and GephE mutant P713E, at 200 nM each. Error bars represent Standard Deviation values. O=PEG linker, ns=non significant, **=p<0.01, ****=p<0,0001. Raw data can be found in Suppl. Fig. 8.

5. DISCUSSION

Protein-protein interactions at the postsynaptic membrane mediate inhibitory synaptic transmission. Gephyrin interaction with the intracellular loops of GlyRs and $GABA_AR$s allow their clustering at postsynaptic densities and is crucial for neurotransmission. Gephyrin-receptor interactions can be modulated by the use of receptor-derived peptides with an optimized design to bind gephyrin with high affinity. This subject has been approached by Maric et al. (2015) regarding GlyR ß and $GABA_AR$ α3 subunits, the two strongest gephyrin binders. The well-conserved gephyrin-binding motif has been explored for both subunits. However, the gephyrin-interaction mechanism of lower affinity binders as GlyR α2 subunit has not been characterised; hence GlyR α2-derived peptides have not been yet conceived. This project aims to validate previous findings on gephyrin-GlyR α2 subunit interactions, and to contribute to elucidate its binding mode.

5.1. Use of Glycine Receptor-Derived Peptides for Competition

Firstly, the high affinity binding of TM3-4 GlyR ß subunit-derived peptides to gephyrin has been recapitulated (Figure 2), as stated formerly (Maric et al., 2015; Maric et al., 2017).

Short dimeric GlyR α2 subunit-derived peptides A2D5 and A2D7 were used for competition with a using a truncation library (Figure 3). Firstly, 5-mer A2D5 suggested a neutralisation effect (Figure 3A). It was expected that the 7-mer A2D7 was a better competitor peptide than A2D5 since its longer sequence is likely to adjust better in gephyrin binding pocket and contribute with additional interactions *via* the ^{370}FN^{371} residues. However, A2D7 did not reach the expected competition even at higher concentration (Figure 3C). The reason behind this is probably a too short sequence of the peptide to fulfill all the interactions at the binding interface that could neutralise gephyrin binding to the peptides of the truncation library. Another possible reason relies on the peptides design, that included two PEG linkers at the C-terminus as spacers between the two parts of the dimer. Probably that is too short and the dimeric conformation cannot fit properly into the GephE dimers.

5.2. Recapitulating Gephyrin-Glycine Receptor α subunits Binding Hierarchy

The truncation scan (Figure 5A) shows that GlyR α2 subunit binds gephyrin with the highest affinity among the GlyR α subunits. These results verify earlier microarray experiments conducted in the Maric group. Furthermore, results show ^{364}VTRESRFNFSGYGMGH^{379} as the strongest binder of GephE among the screened GlyR α2-derived peptides (Figure 5B). Binding intensity drops dramatically from truncation of this peptide at the C-terminal end. Thus, in light of the dimeric peptide A2D7 not reaching the expected neutralisation effect, neighboring amino acids at the C-terminus should be taken into consideration to enlarge the peptide.

Results from the competition assays with DB1D using an overlapping library (Figure 6) show a lower neutralisation effect than in previous experiments at the same concentration. The reason possibly relies peptides solubility. Aggregation and precipitation of the peptide may lead to an actually lower concentration in solution. Disulfide bridge formation by the C-terminus cysteine because of oxidative conditions during the SPPS could explain the aggregation. Nevertheless, results from Figure 5 are in accordance with the truncation scan (Figure 5). They verify the gephyrin binding hierarchy of GlyR α subunits being GlyR α2 subunit the strongest binder. GlyR α2-derived peptides from the library are less sensitive than other GlyR α subunits to the neutralisation effect caused by DB1D, a dimeric GlyR α2-derived competitor peptide. Testint the highest concentration of peptide, accumulative binding intensity decreases around 60 % for GlyR α1, α3 and α4, whereas 40 % for GlyR α2. This means that GephE binds preferentially DB1D –thus, GlyR α2– than the GlyR α1, α3 and α4 peptides in microarray format.

5.3. Profiling of Glycine Receptor α2 Interaction with Gephyrin

Gephyrin most studied binding peptides have residues extremely conserved, especially between GlyR ß and $GABA_AR$ α3 subunits. A gephyrin consensus peptide-binding motif has been established based on peptide array screen and

alignment of fine mapped gephyrin binding sites (Table 1 and 9). Further alignment and position scoring for the GlyR α2 gephyrin-binding hotspot ^{370}FNFSGYG^{376} remain to be done. Still, first glance similarities of the sequence with ^{398}FSIVG^{402} and ^{368}FNIVG^{372} from GlyR ß and GABA$_A$R α3, respectively, indicate suitability for the binding motif. Table 9 shows the gephyrin consensus peptide-binding motif including a suggested alignment for GlyR α2 sequence.

Table 9. Gephyrin consensus peptide-binding motif. Hydrophobic residues (orange) are highly conserved. Adapted from Maric et al. (2017).

	Binding Motif										
Position	0	1	2	3	4	5	6	7	8	9	10
Consensus	Ω	ζ	Ψ	Ψ	G	ζ	x	P/Y	f_c		
GlyR ß	^{398}F	S	I	V	G	S	L	P	R	D	F
GABA$_A$R α1	^{340}Y	A	P	T	A	T	S	Y	T	P	I
GABA$_A$R α2	^{338}A	Y	A	V	A	V	A	N	Y	A	P
GABA$_A$R α3	^{368}F	N	I	V	G	T	T	Y	P	I	N
GABA$_A$R α5	^{379}A	F	T	T	G	D	M	S	H	P	P
GlyR α2	^{370}F	N	F	S	G	Y	G	M	G	H	C

Ω: aromatic, ζ: hydrophilic, Ψ: large aliphatic, x: not conserved,
f_c: flanking ligand core at the C-terminus

The crystal structure of GlyR ß interaction with GephE shown in Figure 1 helps compare and rationalize the FPS interpretation of GlyR α2 gephyrin-binding hotspot.

From the FPS of GlyR α2 (Figure 7), the following observations can be taken into account. Firstly, the second half of the FPS library was designed using two PEG linkers as spacers between the C-terminal amino acids and the cellulose paper, avoiding potential binding interferences. Results (Figure 7, Figure 8) show the same pattern when comparing the binding intensities of the peptides with and without the PEG linkers. In addition, GephE, FL-Geph and native gephyrin from brain lysate bind following the same trend (Figure 7).

Hydrophobic variations increase binding intensities at F370 and F372 (Figure 7C). Hydrophobicity appears to be key for positions 0 and 2, rather than aromaticity of residues in particular, since variation to hydrophobic residues solely (Ala, Ile, Leu, Val) enhance binding as well as hydrophobic and aromatic residues (Trp, Tyr) do. In contrast to GlyR α2, a mutational scan of GlyR ß subunit gephyrin-binding region revealed an enhanced gephyrin binding only when F398 was variated to Tyr (Maric et al., 2017). Altogether, this recapitulates the hydrophobic binding interface of the conserved N-terminal part of the receptor-core binding sites and gephyrin-binding receptors (Maric et al., 2014).

Residue S373 from GlyR α2 subunit accepts negatively charged amino acids in that position (Figure 7C). In comparison to GlyR ß subunit, phosphomimetic studies evidenced that the residue S403 from GlyR ß subunit modulates gephyrin binding since it is a phosphorilation target. The introduction of negatively charged residues with the GlyR ß mutants S403D and S403E mimics phosphorylation at S403. Affinity of the ß-loop-gephyrin interaction was considerably lowered (Specht et al., 2011). Instead, S373D variation at the GlyR α2 subunit gephyrin-binding sequence increases gephyrin binding. The residue S373 of the GlyR α2 was shown to be a phosphorilation site (Huttlin et al., 2010). It can thus be hypothethised that S373 also plays a role in the regulation of affinity binding to gephyrin through phosphorilation. However, an opposite effect might be caused, thus pointing out potentially differential functions of GlyR subunits upon gephyrin binding.

The position 4 in the GlyR ß loop motif only accepts Gly (G402). Variation to any other amino acid in microarray format results in completely abolished gephyrin binding because conformational flexibility for tight interface contact is required. Interestingly, the corresponding residues in $GABA_AR$ α1 and α3 (A344 and G372, respectively) are also very small (Maric et al., 2011; Maric et al., 2017). A glycine (G374) is also found at the corresponding position of GlyR α2 hotspot. However, G374 seems not to be as conserved since other residues are accepted as well (Figure 7C). This could point towards the GlyR α2 subunit binding in a partly overlapping yet not entirely identical binding pocket.

The most notable observation from the GlyR α2 hotspot FPS is that only Y375 is accepted in this position, while a variation to any other amino acid abolishes binding. Remarkably, a variation to phenylalanine is not tolerated in that position either. Therefore, the hydroxyl group from the tyrosine side chain might play a role through additional interactions like hydrogen-bonding formation. Tyrosine has an amphipathic side chain capable of forming cation-π interactions and non-polar hydrogen bonds. Its physicochemical character contributes to high affinity and specificity at the binding interface (Koide et al., 2009). As a comparison to GlyR ß subunit, gephyrin Tyr673 and Asp327 residues are known to form hydrogen bonds with Ser399 of GlyR ß subunit (Maric et al., 2014), that represents position 1 from the gephyrin consensus peptide-binding motif (Table 9). Correspondingly, Tyr375 from GlyR α2 subunit fits nearby and is likely to form hydrogen bonds with those gephyrin residues. It is also noteworthy that hotspots in binding interfaces, that tend to be intolerant to substitutions, are usually particularly enriched in tyrosine (Koide et al., 2009).

The FPS of the GlyR α2 hotspot using GephE mutants F330A and P713E (Eun et al., 2006) (Figure 9) untangles the protein-peptide interaction mode with high molecular detail. Results from the positional scan using GephE wild-type (Figures 7A, 7C, 7A, 7C) follow a similar pattern. A similar pattern can also be observed comparing the heatmaps of sequences with and without PEG linkers (Figures 9A, 9D; 9B, 9E; 9C, 9F).

The mutation P713E in GephE abolishes binding to GlyR ß, $GABA_AR$ α1 and $GABA_AR$ α3 subunits due to a steric blocking of the predicted peptide binding site by introducing a bulky and negatively charged side chain in the otherwise constrained and hydrophobic binding pocket. Besides, the mutation F330A at the N-terminal region of the GephE peptide binding region weakens binding intensity for GlyR ß-derived peptides by reducing the contribution of a critical π-π stacking, thus impairing aromatic interactions. Nevertheless, some peptide variants with large hydrophobic residues in the F330 binding region compensate the loss of N-terminal interaction surface (Maric et al., 2017). This effect has also been observed regarding $GABA_AR$ α1 and $GABA_AR$ α3 subunits (Maric et al., 2011).

In stark contrast, GephE P713E mutation slightly diminishes binding with GlyR α2 subunit (Figure 10). This leads to considering a different binding mechanism between GlyR ß and GlyR α2 subunits. While GlyR ß and $GABA_AR$ α3-binding sites overlap significantly and are mutually exclusive (Maric et al., 2014), a partially overlapping binding site of GlyR α2 within the N-terminal part of the receptor core-binding site can be postulated.

Residues interacting with GephE F330 are highly conserved among GlyRß, $GABA_AR$ α3 and GlyR α2 subunits. The GephE F330A mutant significantly decreases binding affinity (Figure 10), and involves a loss of hydrophobicity and aromaticity at the interface. Binding could be compensated by the introduction other hydrophobic side chains by GlyR α2 peptide variants from the FPS library (Figure 9B). π-π stacking interactions between GephE F330 and GlyR ß subunit F398 have been crystallographically resolved (Maric et al., 2011). Due to the conserved residue in the corresponding position, a similar binding mechanism could take place between GephE F330 and either GlyR α2 subunit F370 or F372. Simetrical peculiarity of the tested sequence ^{370}FNFSGYG^{376} regarding the Phe and the Gly positions allow shifting to the left the alignment and still fit into the proposed consensus motif (Table 9). This fact is reflected in the similar pattern of the intensities for columns of the heatmap corresponding to F370 and F372, and to G374 and G376 (Figure 9E).

Surprisingly, variation to Tyr at F372 position enhances binding in comparison to the wild-type peptide (Figure 9). The same stacking interactions between GlyR α2 phenylalanines and GephE F330 may not take place with GephE F330A mutant. As discussed previously for Figure 6, variations to tyrosine are likely to compensate this occupying the place of Phe330 side chain and by forming additional interactions through its reacting hydroxyl group. Taken as a whole, variation to tyrosine enhances binding at almost any position of the binding motif, which upholds the importance of this residue at gephyrin-GlyR α2 binding interface.

It Is also noticeable that Pro and Tyr are well accepted at the G376 position (Figure 9B). Variations to these residues resemble the proposed consensus motif

for GlyR ß subunit (Pro at position 7) and for $GABA_AR$ α1 and α3 subunits (conserved Try at position 7). Finally, mutations to positively charged amino acids at physiological pH (Arg, Lys) abolish binding completely (Figure 7, 9).

Competiton assay with the 7-mer GlyR α2-derived dimeric peptide "A2D7" using the FPS library (Figure 8) did not show the desired neutralisation effect although the peptide was competing for gephyrin binding with peptide variants of similar sequence. The tested GlyR α2 peptide might be too short also on that basis.

In the work Characterisation of Glycine Receptor α Subunit Interactions with Gephyrin, by David Baumstark (2021), ^{372}FSGYGM^{377} was defined as GlyR α2 minimal fragment. However, results presented in this project show that GlyR α2 minimal fragment could be reconsidered and maybe enlarged. Based on the results using the short GlyR α2-derived competitor peptides, appropiate peptides for crystalization should be longer than 7 amino acids preferably enlarged at the C-terminus, but shorter than 15 amino acids to circumvent peptide aggregation and enhance solubility. The peptide could be enlarged at the C-terminus by including the ^{377}MGH^{379} residues, which is also suggested from the truncation scan results. Regardless of binding contribution, the C-terminal hystidine is expected to enhance solubulity of the peptide, together with two PEG linkers included in the architecture of the dimeric peptide. Following amino acid Cys380 will not be suitably included due to possible sulfide bonds formation that promote aggregation, as has been postulated for the 15-mer DB1D peptide. Due to the symmetry of the sequence, ^{370}FN^{371} may or may not be critical for binding. Therefore, peptide synthesis onwards could include or not these residues to discern their importance.

The peptide that achieves good binding to gephyrin by competition assays is candidate to become a crystal structure. X-ray crystal structures of the GlyR α2 peptide would be useful to resolve its binding mode. Further details about GlyR α2 peptides could be assimilated by quantification of their biophysical properties and binding affinity by isothermal titration calorimetry and bio-layer interferometry.

6. CONCLUSION

Interactions between gephyrin and GlyR can be explored to further elucidate the modulation of inhibitory postsynapse. So far, the scientific community has put ahead GlyR ß binding to gephyrin and ignored other possibilities of GlyR-gephyrin binding considering embryonic homomeric receptors only formed by GlyR α2 subunits. GlyR α2 subunit interactions with gephyrin were attempted to be puzzled out within this project.

This project recapitulates the high affinity binding of GlyR ß subunit to gephyrin through neutralisation assays with the minimum GlyR ß-derived gephyrin-binding peptide. Moreover, truncational scan results showed GlyR α2 as the strongest binder among GlyR α subunits. Thus, gephyrin binding hierarchy is confirmed by GlyR α2 being the third stronger gephyrin binder.

On-chip peptide neutralisation assays with GlyR α2-derived dimeric peptides aimed to test reproducibility of previous studies. The 15-mer peptide failed to achieve the expected competition, probably due to aggregation. The 7-mer ^{370}FNFSGYG^{376} displayed good binding to gephyrin when immobilized on the array (binding assays with the FPS library), albeit not the desired outcome in soluble format (dimeric competitor peptide). Complementary experiments with truncational and full positional libraries suggested this sequence as too short. FPS of GlyR α2 gephyrin binding hotspot attempted to assess the contribution of the residues ^{370}FNFSGYG^{376} to binding. As main highlights, Y375 and hydrophobicity at F370 and F372 positions seem key. It can be suggested that GlyR α2 and stronger gephyrin binders share a partially overlapping binding site.

Future studies could promisingly focus on the synthesis of a longer GlyR α2-derived peptide, ideally a 10-mer including ^{370}FNFSGYGMGH^{379}, or a 8-mer including ^{372}FSGYGMGH^{379}. Peptide elongation at the C-terminus seems necessary. A comparison between both peptide candidates can be done to evaluate the importance of the ^{370}FN^{371} residues.

To sum up, the cutting edge this project reveals is GlyR α2 binding in a specific manner to gephyrin. As a clear example, binding of GlyR α2 to gephyrin was impaired only with the GephE single point mutation F330A.

REFERENCES

Alvarez FJ. Gephyrin and the regulation of synaptic strength and dynamics at glycinergic inhibitory synapses. Brain Res Bull. 2017;129:50–65.

Eun YK, Schrader N, Smolinsky B, Bedet C, Vannier C, Schwarz G, et al. Deciphering the structural framework of glycine receptor anchoring by gephyrin. EMBO J. 2006;25(6):1385–95.

Groeneweg FL, Trattnig C, Kuhse J, Nawrotzki RA, Kirsch J. Gephyrin: a key regulatory protein of inhibitory synapses and beyond. Histochem Cell Biol. 2018;150(5):489–508.

Huttlin EL, Jedrychowski MP, Elias JE, Goswami T, Rad R, Beausoleil SA, et al. A tissue-specific atlas of mouse protein phosphorylation and expression. Cell. 2010;143(7):1174–89.

Kirsch J, Wolters I, Triller A, Betz H. Gephyrin antisense oligonucleotides prevent glycine receptor clustering in spinal neurons. Nature. 1993;366(6457):745–8.

Kneussel M, Brandstätter JH, Laube B, Stahl S, Müller U, Betz H. Loss of postsynaptic GABA(A) receptor clustering in gephyrin-deficient mice. J Neurosci. 1999;19(21):9289–97.

Koide, S; Sidhu SS. The Importance of Being Tyrosine: Lessons in Molecular Recognition from Minimalist Synthetic Binding Proteins. ACS Chem Biol. 2009;4(5):325–34.

Langlhofer G, Villmann C. The intracellular loop of the glycine receptor: It's not all about the size. Front Mol Neurosci. 2016;9(41):1–14.

Maas C, Tagnaouti N, Loebrich S, Behrend B, Lappe-Siefke C, Kneussel M. Neuronal cotransport of glycine receptor and the scaffold protein gephyrin. J Cell Biol. 2006;172(3):441–51.

Maric HM, Hausrat TJ, Neubert F, Dalby NO, Doose S, Sauer M, et al. Gephyrin-binding peptides visualize postsynaptic sites and modulate neurotransmission. Nat Chem Biol. 2017;13(2):153–60.

Maric HM, Kasaragod VB, Haugaard-Kedström L, Hausrat TJ, Kneussel M, Schindelin H, et al. Design and synthesis of high-affinity dimeric inhibitors targeting the interactions between gephyrin and inhibitory neurotransmitter receptors. Angew Chemie - Int Ed. 2015;54(2):490–4.

Maric HM, Kasaragod VB, Hausrat TJ, Kneussel M, Tretter V, Strømgaard K, et al. Molecular basis of the alternative recruitment of GABAA versus glycine receptors through gephyrin. Nat Commun. 2014;5:1–11.

Maric HM, Mukherjee J, Tretter V, Moss SJ, Schindelin H. Gephyrin-mediated γ-aminobutyric acid type A and glycine receptor clustering relies on a common binding site. J Biol Chem. 2011;286(49):42105–14.

San Martín VP, Sazo A, Utreras E, Moraga-Cid G, Yévenes GE. Glycine Receptor Subtypes and Their Roles in Nociception and Chronic Pain. Front Mol Neurosci. 2022;15(848642):1–9.

Schaefer N, Vogel N, Villmann C. Glycine receptor mutants of the mouse: What are possible routesof inhibitory compensation? Front Mol Neurosci. 2012;5(98):1–16.

Schrader N, Kim EY, Winking J, Paulukat J, Schindelin H, Schwarz G. Biochemical Characterization of the High Affinity Binding between the Glycine Receptor and Gephyrin. J Biol Chem. 2004;279(18):18733–41.

Specht CG, Grünewald N, Pascual O, Rostgaard N, Schwarz G, Triller A. Regulation of glycine receptor diffusion properties and gephyrin interactions by protein kinase C. EMBO J. 2011;30(18):3842–53.

Tyagarajan SK, Fritschy JM. Gephyrin: A master regulator of neuronal function? Nat Rev Neurosci. 2014;15(3):141–56.

Yu H, Bai XC, Wang W. Characterization of the subunit composition and structure of adult human glycine receptors. Neuron. 2021;109(17):2707-16.

Zhu H, Gouaux E. Architecture and assembly mechanism of native glycine receptors. Nature. 2021;599(7885):513–7.

SELF-ASSESSMENT

The development of my Final Degree Project during the internship at AG Maric has been a great opportunity for discovering a novel technology applied to an understudied area of research. Because it was the first time I was involved in a peptide synthesis-related project, I researched about it and soaked up new concepts. I was also taught new technical skills regarding working with peptide microarrays. Then I could work autonomously, which sometimes was challenging for me in terms of taking decisions during the experiments. Nevertheless, I was always encouraged to ask questions and resolve my doubts, not only during practical work but also about theoretical background.

As a take-home message, I learnt to take advice and constructive criticism from weekly meetings, and manage my time; until now I was not aware that lab time, results-analysis time and writing time have to be that well balanced, otherwise one cannot continue their project if some are missing. All in all, this experience has been a huge educational trip towards developing my scientific career.

ACKNOWLEDGMENTS

I am truly thankful to Dr. Hans Michael Maric for the opportunity of doing my bachelor's thesis in his lab, to Clemens Schulte for guiding and advising me during my stay, and to the whole Maric group for welcoming me and for their helpful feedback. Finally, I want to thank my family for being always my biggest support.

SUPPLEMENTARY DATA

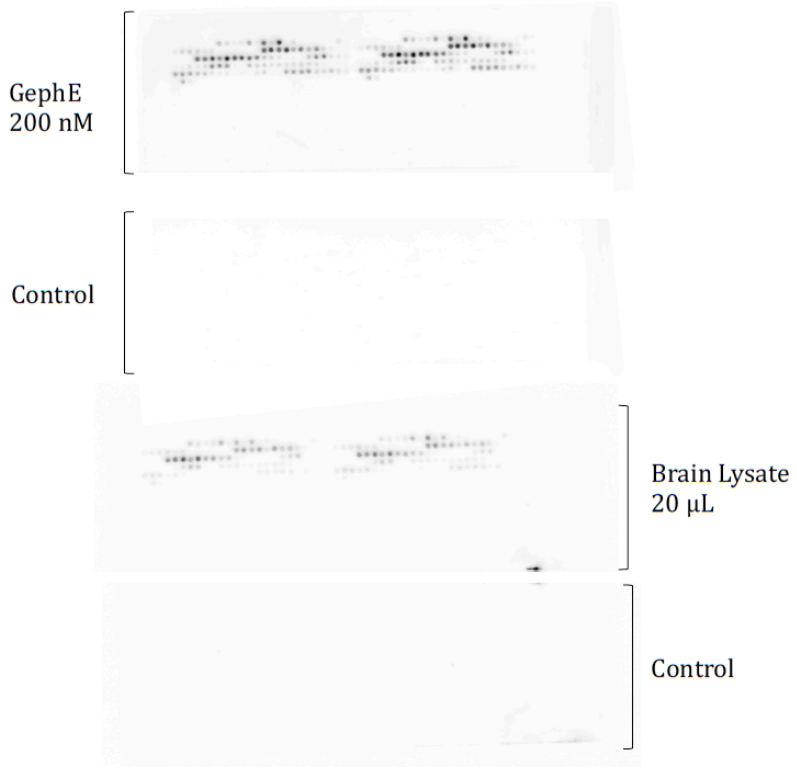

Supplementary figure 1. Raw data of binding assay with GephE at 200 nM and 20 µL of mouse brain lysate and using a truncation library with gephyrin-binding sequences from GlyR α subunits.

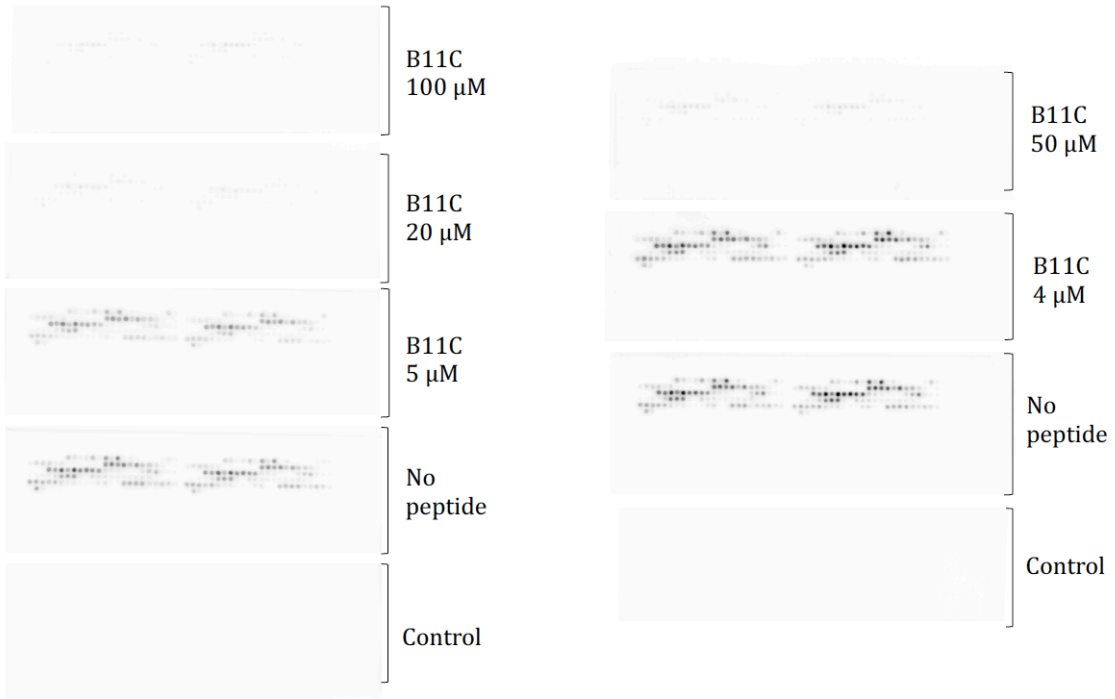

Supplementary figure 2. Raw data of neutralisation assay with GlyR ß subunit-derived competitor peptide B11C, GephE at 200 nM and using a truncation library with gephyrin-binding sequences from GlyR α subunits.

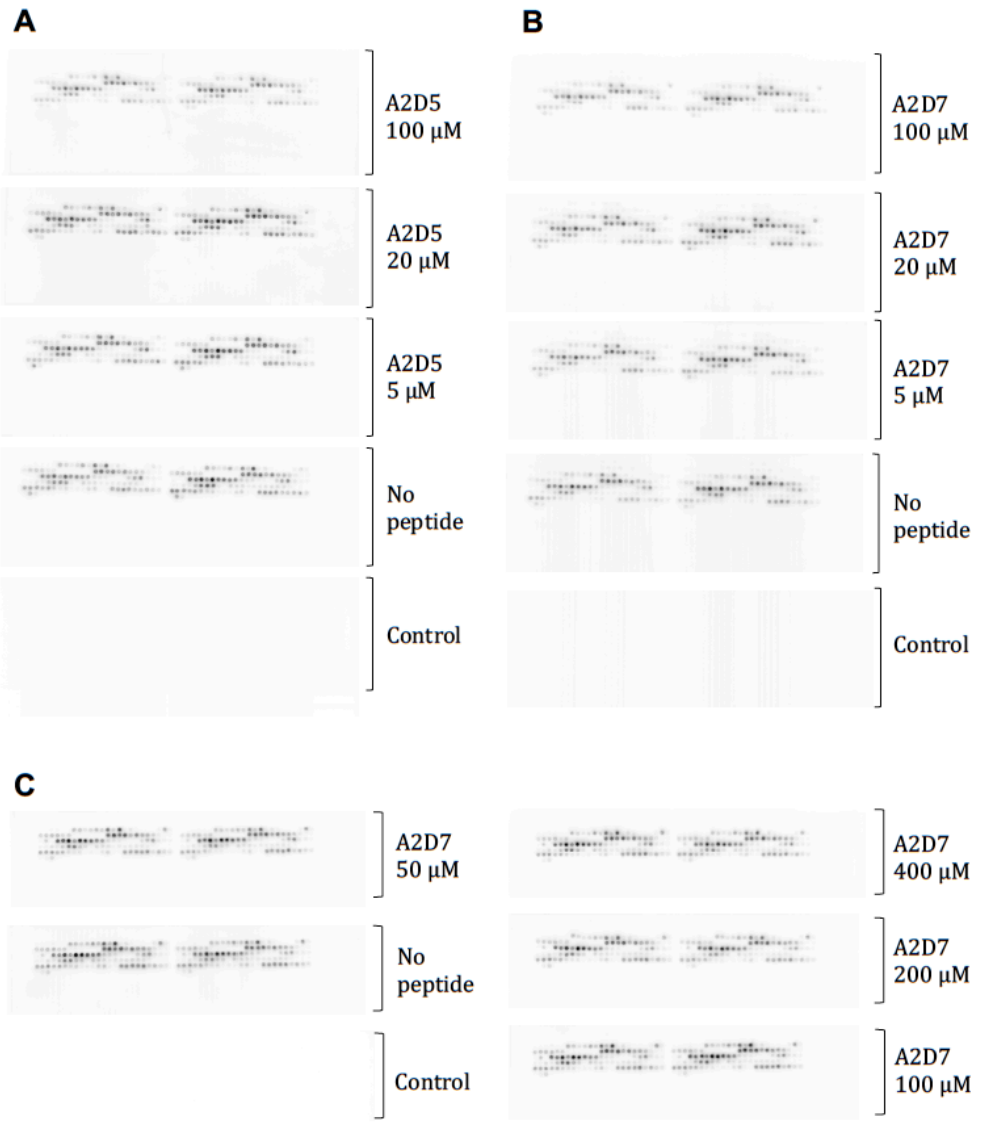

Supplementary figure 3. Raw data of neutralisation assay on truncation library with gephyrin-binding sequences from GlyR α subunits, using GephE at 200 nM and (A) 5-mer GlyR α2-derived dimeric peptide A2D5 at 5, 20 and 100 µM; (B) 7-mer GlyR α2-derived dimeric peptide A2D7 at 5, 20 and 100 µm; (C) A2D7 at 50, 100, 200 and 400 µM as competitor peptides.

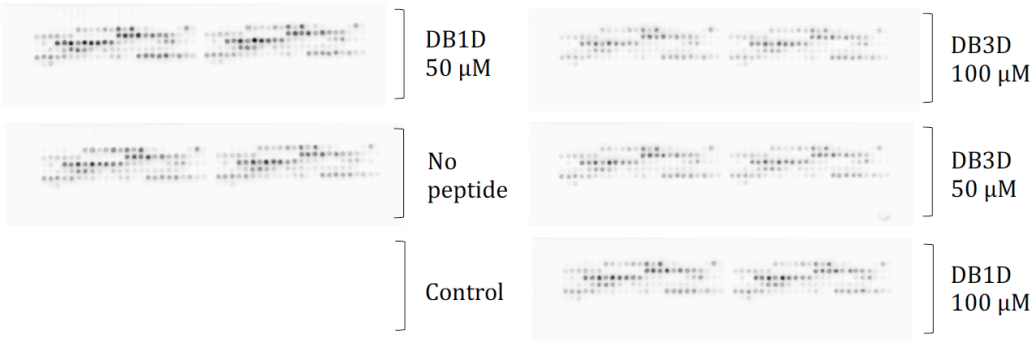

Supplementary figure 4. Raw data of neutralisation assay on truncation library with gephyrin-binding sequences from GlyR α subunits, using DB1D and DB3D at 50 and 100 µM each as competitor peptide and negative control, respectively, and GephE at 200 nM.

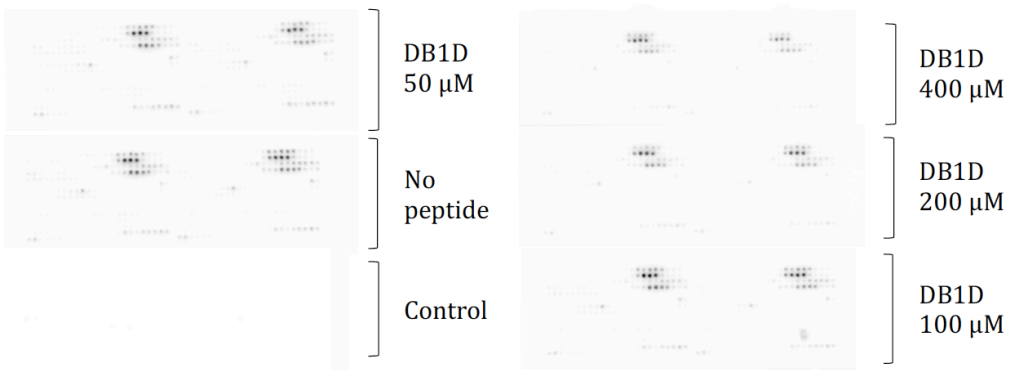

Supplementary figure 5. Raw data of neutralisation assay on a $GABA_AR$/GlyR α overlapping library, using DB1D as competitor peptide and GephE at 200 nM.

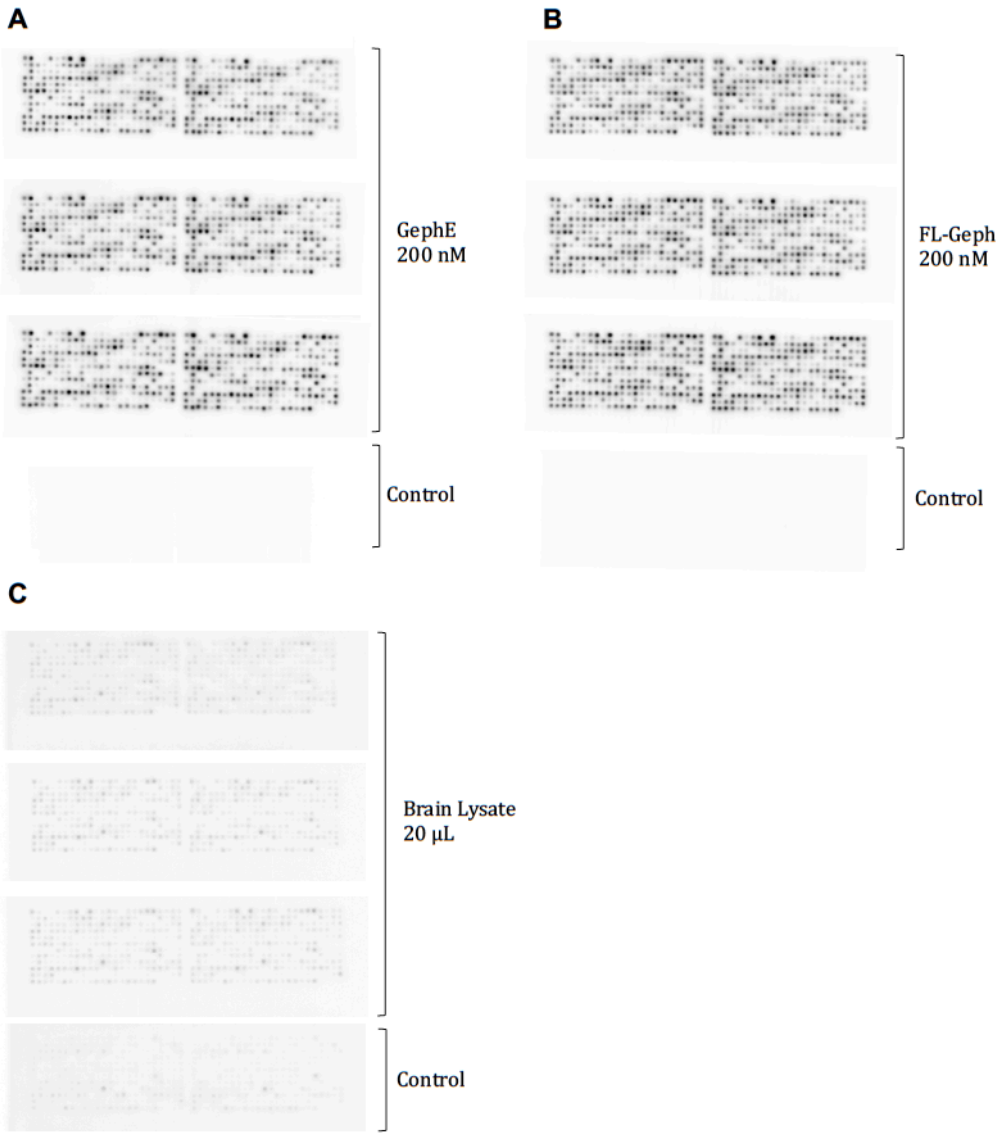

Supplementary figure 6. Raw data of binding assay on a GlyR α2 FPS library using (A) GephE at 200 nM, (B) FL-Geph at 200 nM, and (C) 20 µL of native gephyrin from brain lysate.

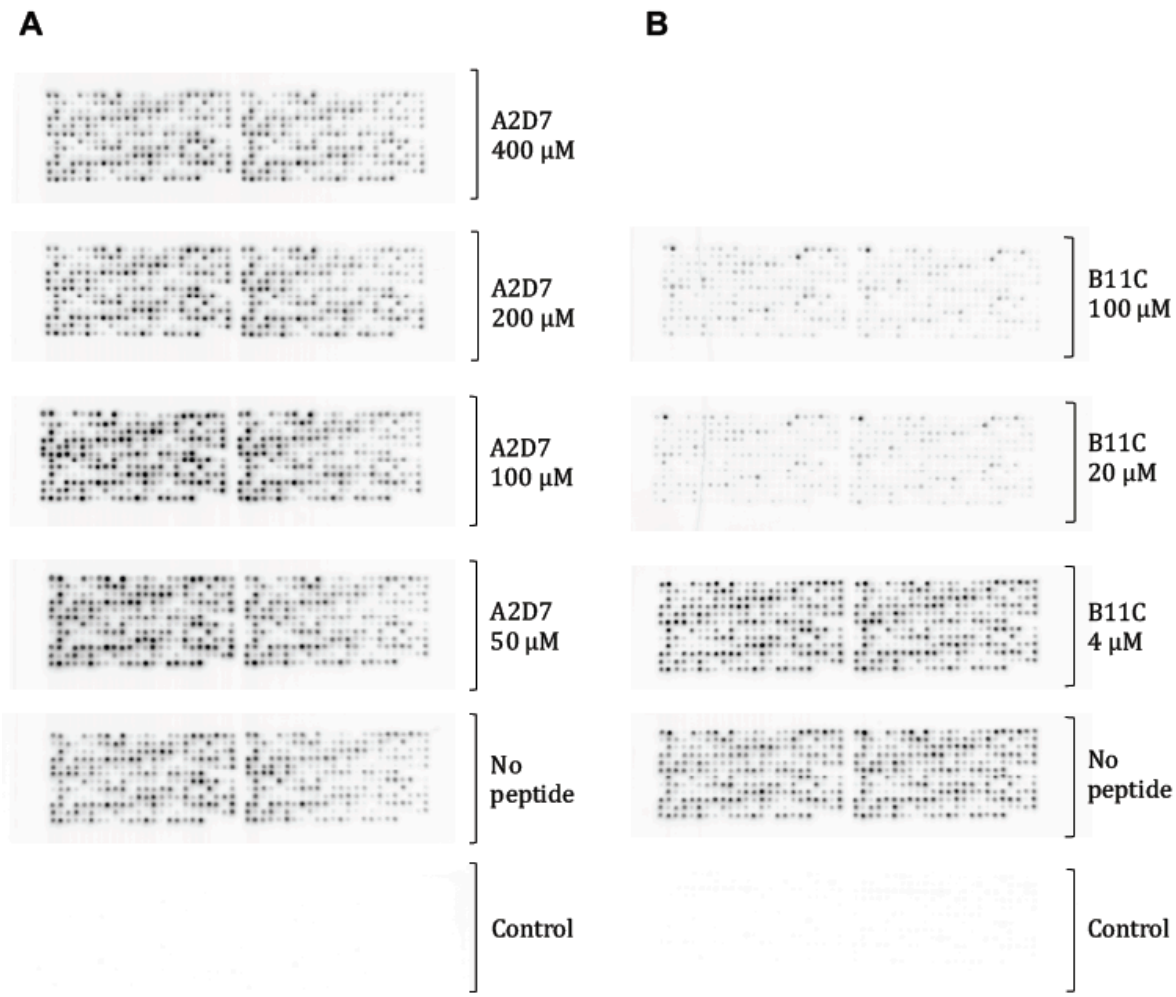

Supplementary figure 7. Raw data of neutralisation assay on a GlyR α2 FPS library, using GephE at 200 nM and (A) A2D7; (B) B11C as competitor peptides.

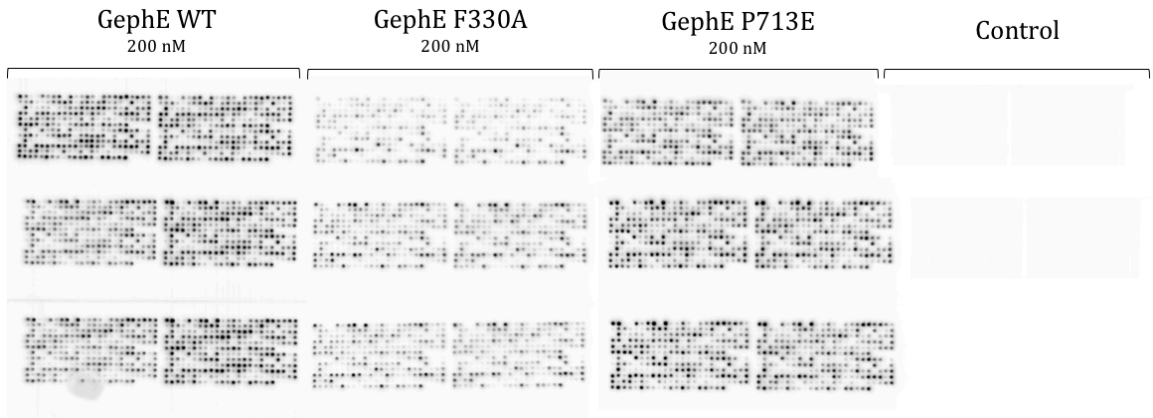

Supplementary figure 8. Raw data of binding assay on a GlyR α2 FPS library using GephE WT, and GephE point mutants F330A and P713E, at 200 nM each.

Supplementary table 1. Truncation scan library. Peptides correspond to the gephyrin-binding sequences of GlyR α subunits.

Position	Sequence Name	Uniprot correspondence	Peptide Sequence
A7	GlyR_A1	>sp|Q64018|364-383	**EGGEGRFNFSAYGMGPACLQ**
A8	GlyR_A1	>sp|Q64018|364-383	EGGEGRFNFSAYGMGPACL
A9	GlyR_A1	>sp|Q64018|364-383	EGGEGRFNFSAYGMGPAC
A10	GlyR_A1	>sp|Q64018|364-383	EGGEGRFNFSAYGMGPA
A11	GlyR_A1	>sp|Q64018|364-383	EGGEGRFNFSAYGMGP
A12	GlyR_A1	>sp|Q64018|364-383	EGGEGRFNFSAYGMG
A13	GlyR_A1	>sp|Q64018|364-383	EGGEGRFNFSAYGM
A14	GlyR_A1	>sp|Q64018|364-383	EGGEGRFNFSAYG
A15	GlyR_A1	>sp|Q64018|364-383	EGGEGRFNFSAY
A16	GlyR_A1	>sp|Q64018|364-383	EGGEGRFNFSA
A17	GlyR_A1	>sp|Q64018|364-383	EGGEGRFNFS
A18	GlyR_A1	>sp|Q64018|364-383	EGGEGRFNF
A19	GlyR_A1	>sp|Q64018|364-383	EGGEGRFN
A20	GlyR_A1	>sp|Q64018|364-383	EGGEGRF
A21	GlyR_A1	>sp|Q64018|364-383	EGGEGR
A22	GlyR_A1	>sp|Q64018|364-383	**EGGEGRFNFSAYGMGPACLQ**
A23	GlyR_A1	>sp|Q64018|364-383	GGEGRFNFSAYGMGPACLQ
A24	GlyR_A1	>sp|Q64018|364-383	GEGRFNFSAYGMGPACLQ
B1	GlyR_A1	>sp|Q64018|364-383	EGRFNFSAYGMGPACLQ
B2	GlyR_A1	>sp|Q64018|364-383	GRFNFSAYGMGPACLQ
B3	GlyR_A1	>sp|Q64018|364-383	RFNFSAYGMGPACLQ
B4	GlyR_A1	>sp|Q64018|364-383	FNFSAYGMGPACLQ
B5	GlyR_A1	>sp|Q64018|364-383	NFSAYGMGPACLQ
B6	GlyR_A1	>sp|Q64018|364-383	FSAYGMGPACLQ
B7	GlyR_A1	>sp|Q64018|364-383	SAYGMGPACLQ
B8	GlyR_A1	>sp|Q64018|364-383	AYGMGPACLQ
B9	GlyR_A1	>sp|Q64018|364-383	YGMGPACLQ
B10	GlyR_A1	>sp|Q64018|364-383	GMGPACLQ
B11	GlyR_A1	>sp|Q64018|364-383	MGPACLQ
B12	GlyR_A1	>sp|Q64018|364-383	GPACLQ
B13	GlyR_A2	>sp|Q7TNC8|364-383	**VTRESRFNFSGYGMGHCLQM**
B14	GlyR_A2	>sp|Q7TNC8|364-383	TRESRFNFSGYGMGHCLQM

B15	GlyR_A2	>sp|Q7TNC8|364-383	RESRFNFSGYGMGHCLQM
B16	GlyR_A2	>sp|Q7TNC8|364-383	ESRFNFSGYGMGHCLQM
B17	GlyR_A2	>sp|Q7TNC8|364-383	SRFNFSGYGMGHCLQM
B18	GlyR_A2	>sp|Q7TNC8|364-383	RFNFSGYGMGHCLQM
B19	GlyR_A2	>sp|Q7TNC8|364-383	FNFSGYGMGHCLQM
B20	GlyR_A2	>sp|Q7TNC8|364-383	NFSGYGMGHCLQM
B21	GlyR_A2	>sp|Q7TNC8|364-383	FSGYGMGHCLQM
B22	GlyR_A2	>sp|Q7TNC8|364-383	SGYGMGHCLQM
B23	GlyR_A2	>sp|Q7TNC8|364-383	GYGMGHCLQM
B24	GlyR_A2	>sp|Q7TNC8|364-383	YGMGHCLQM
C1	GlyR_A2	>sp|Q7TNC8|364-383	GMGHCLQM
C2	GlyR_A2	>sp|Q7TNC8|364-383	MGHCLQM
C3	GlyR_A2	>sp|Q7TNC8|364-383	GHCLQM
C4	GlyR_A2	>sp|Q7TNC8|364-383	**VTRESRFNFSGYGMGHCLQM**
C5	GlyR_A2	>sp|Q7TNC8|364-383	VTRESRFNFSGYGMGHCLQ
C6	GlyR_A2	>sp|Q7TNC8|364-383	VTRESRFNFSGYGMGHCL
C7	GlyR_A2	>sp|Q7TNC8|364-383	VTRESRFNFSGYGMGHC
C8	GlyR_A2	>sp|Q7TNC8|364-383	VTRESRFNFSGYGMGH
C9	GlyR_A2	>sp|Q7TNC8|364-383	VTRESRFNFSGYGMG
C10	GlyR_A2	>sp|Q7TNC8|364-383	VTRESRFNFSGYGM
C11	GlyR_A2	>sp|Q7TNC8|364-383	VTRESRFNFSGYG
C12	GlyR_A2	>sp|Q7TNC8|364-383	VTRESRFNFSGY
C13	GlyR_A2	>sp|Q7TNC8|364-383	VTRESRFNFSG
C14	GlyR_A2	>sp|Q7TNC8|364-383	VTRESRFNFS
C15	GlyR_A2	>sp|Q7TNC8|364-383	VTRESRFNF
C16	GlyR_A2	>sp|Q7TNC8|364-383	VTRESRFN
C17	GlyR_A2	>sp|Q7TNC8|364-383	VTRESRF
C18	GlyR_A2	>sp|Q7TNC8|364-383	VTRESR
C19	GlyR_A3	>sp|Q91XP5|366-385	**FYRFSDTDDEVRESRFSFTA**
C20	GlyR_A3	>sp|Q91XP5|366-385	FYRFSDTDDEVRESRFSFT
C21	GlyR_A3	>sp|Q91XP5|366-385	FYRFSDTDDEVRESRFSF
C22	GlyR_A3	>sp|Q91XP5|366-385	FYRFSDTDDEVRESRFS
C23	GlyR_A3	>sp|Q91XP5|366-385	FYRFSDTDDEVRESRF
C24	GlyR_A3	>sp|Q91XP5|366-385	FYRFSDTDDEVRESR
D1	GlyR_A3	>sp|Q91XP5|366-385	FYRFSDTDDEVRES

D2	GlyR_A3	>sp|Q91XP5|366-385	FYRFSDTDDEVRE
D3	GlyR_A3	>sp|Q91XP5|366-385	FYRFSDTDDEVR
D4	GlyR_A3	>sp|Q91XP5|366-385	FYRFSDTDDEV
D5	GlyR_A3	>sp|Q91XP5|366-385	FYRFSDTDDE
D6	GlyR_A3	>sp|Q91XP5|366-385	FYRFSDTDD
D7	GlyR_A3	>sp|Q91XP5|366-385	FYRFSDTD
D8	GlyR_A3	>sp|Q91XP5|366-385	FYRFSDT
D9	GlyR_A3	>sp|Q91XP5|366-385	FYRFSD
D10	GlyR_A3	>sp|Q91XP5|366-385	**FYRFSDTDDEVRESRFSFTA**
D11	GlyR_A3	>sp|Q91XP5|366-385	YRFSDTDDEVRESRFSFTA
D12	GlyR_A3	>sp|Q91XP5|366-385	RFSDTDDEVRESRFSFTA
D13	GlyR_A3	>sp|Q91XP5|366-385	FSDTDDEVRESRFSFTA
D14	GlyR_A3	>sp|Q91XP5|366-385	SDTDDEVRESRFSFTA
D15	GlyR_A3	>sp|Q91XP5|366-385	DTDDEVRESRFSFTA
D16	GlyR_A3	>sp|Q91XP5|366-385	TDDEVRESRFSFTA
D17	GlyR_A3	>sp|Q91XP5|366-385	DDEVRESRFSFTA
D18	GlyR_A3	>sp|Q91XP5|366-385	DEVRESRFSFTA
D19	GlyR_A3	>sp|Q91XP5|366-385	EVRESRFSFTA
D20	GlyR_A3	>sp|Q91XP5|366-385	VRESRFSFTA
D21	GlyR_A3	>sp|Q91XP5|366-385	RESRFSFTA
D22	GlyR_A3	>sp|Q91XP5|366-385	ESRFSFTA
D23	GlyR_A3	>sp|Q91XP5|366-385	SRFSFTA
D24	GlyR_A3	>sp|Q91XP5|366-385	RFSFTA
E1	GlyR_A4	>sp|Q2TB05|324-343	**IIRESRFYFRGYGLGHCLQA**
E2	GlyR_A4	>sp|Q2TB05|324-343	IIRESRFYFRGYGLGHCLQ
E3	GlyR_A4	>sp|Q2TB05|324-343	IIRESRFYFRGYGLGHCL
E4	GlyR_A4	>sp|Q2TB05|324-343	IIRESRFYFRGYGLGHC
E5	GlyR_A4	>sp|Q2TB05|324-343	IIRESRFYFRGYGLGH
E6	GlyR_A4	>sp|Q2TB05|324-343	IIRESRFYFRGYGLG
E7	GlyR_A4	>sp|Q2TB05|324-343	IIRESRFYFRGYGL
E8	GlyR_A4	>sp|Q2TB05|324-343	IIRESRFYFRGYG
E9	GlyR_A4	>sp|Q2TB05|324-343	IIRESRFYFRGY
E10	GlyR_A4	>sp|Q2TB05|324-343	IIRESRFYFRG
E11	GlyR_A4	>sp|Q2TB05|324-343	IIRESRFYFR
E12	GlyR_A4	>sp|Q2TB05|324-343	IIRESRFYF

E13	GlyR_A4	>sp|Q2TB05|324-343	IIRESRFY
E14	GlyR_A4	>sp|Q2TB05|324-343	IIRESRF
E15	GlyR_A4	>sp|Q2TB05|324-343	IIRESR
E16	GlyR_A4	>sp|Q2TB05|324-343	**IIRESRFYFRGYGLGHCLQA**
E17	GlyR_A4	>sp|Q2TB05|324-343	IRESRFYFRGYGLGHCLQA
E18	GlyR_A4	>sp|Q2TB05|324-343	RESRFYFRGYGLGHCLQA
E19	GlyR_A4	>sp|Q2TB05|324-343	ESRFYFRGYGLGHCLQA
E20	GlyR_A4	>sp|Q2TB05|324-343	SRFYFRGYGLGHCLQA
E21	GlyR_A4	>sp|Q2TB05|324-343	RFYFRGYGLGHCLQA
E22	GlyR_A4	>sp|Q2TB05|324-343	FYFRGYGLGHCLQA
E23	GlyR_A4	>sp|Q2TB05|324-343	YFRGYGLGHCLQA
E24	GlyR_A4	>sp|Q2TB05|324-343	FRGYGLGHCLQA
F1	GlyR_A4	>sp|Q2TB05|324-343	RGYGLGHCLQA
F2	GlyR_A4	>sp|Q2TB05|324-343	GYGLGHCLQA
F3	GlyR_A4	>sp|Q2TB05|324-343	YGLGHCLQA
F4	GlyR_A4	>sp|Q2TB05|324-343	GLGHCLQA
F5	GlyR_A4	>sp|Q2TB05|324-343	LGHCLQA
F6	GlyR_A4	>sp|Q2TB05|324-343	GHCLQA

Supplementary table 2. Overlapping library. Peptides correspond to the TM3-4 loop of GABAAR α, GABAAR γ1, and GlyR subunits, except GlyR ß and GABAAR α3.

Position	Sequence Name	Uniprot correspondence	Peptide Sequence
A7	GlyR_A1	>sp|Q64018|331-425	AVNFVSRQHKELLRFRRKRR
A8	GlyR_A1	>sp|Q64018|331-425	FVSRQHKELLRFRRKRRHHK
A9	GlyR_A1	>sp|Q64018|331-425	RQHKELLRFRRKRRHHKSPM
A10	GlyR_A1	>sp|Q64018|331-425	KELLRFRRKRRHHKSPMLNL
A11	GlyR_A1	>sp|Q64018|331-425	LRFRRKRRHHKSPMLNLFQD
A12	GlyR_A1	>sp|Q64018|331-425	RRKRRHHKSPMLNLFQDDEG
A13	GlyR_A1	>sp|Q64018|331-425	RRHHKSPMLNLFQDDEGGEG
A14	GlyR_A1	>sp|Q64018|331-425	HKSPMLNLFQDDEGGEGRFN
A15	GlyR_A1	>sp|Q64018|331-425	PMLNLFQDDEGGEGRFNFSA
A16	GlyR_A1	>sp|Q64018|331-425	NLFQDDEGGEGRFNFSAYGM
A17	GlyR_A1	>sp|Q64018|331-425	QDDEGGEGRFNFSAYGMGPA
A18	GlyR_A1	>sp|Q64018|331-425	EGGEGRFNFSAYGMGPACLQ
A19	GlyR_A1	>sp|Q64018|331-425	EGRFNFSAYGMGPACLQAKD

A20	GlyR_A1	>sp|Q64018|331-425	FNFSAYGMGPACLQAKDGIS
A21	GlyR_A1	>sp|Q64018|331-425	SAYGMGPACLQAKDGISVKG
A22	GlyR_A1	>sp|Q64018|331-425	GMGPACLQAKDGISVKGANN
A23	GlyR_A1	>sp|Q64018|331-425	PACLQAKDGISVKGANNNNT
A24	GlyR_A1	>sp|Q64018|331-425	LQAKDGISVKGANNNNTTNP
B1	GlyR_A1	>sp|Q64018|331-425	KDGISVKGANNNNTTNPPPA
B2	GlyR_A1	>sp|Q64018|331-425	ISVKGANNNNTTNPPPAPSK
B3	GlyR_A1	>sp|Q64018|331-425	KGANNNNTTNPPPAPSKSPE
B4	GlyR_A1	>sp|Q64018|331-425	NNNNTTNPPPAPSKSPEEMR
B5	GlyR_A1	>sp|Q64018|331-425	NTTNPPPAPSKSPEEMRKLF
B6	GlyR_A1	>sp|Q64018|331-425	NPPPAPSKSPEEMRKLFIQR
B7	GlyR_A1	>sp|Q64018|331-425	PAPSKSPEEMRKLFIQRAKK
B8	GlyR_A1	>sp|Q64018|331-425	SKSPEEMRKLFIQRAKKIDK
B9	GlyR_A2	>sp|Q7TNC8|337-420	AVNFVSRQHKEFLRLRRRQK
B10	GlyR_A2	>sp|Q7TNC8|337-420	FVSRQHKEFLRLRRRQKRQN
B11	GlyR_A2	>sp|Q7TNC8|337-420	RQHKEFLRLRRRQKRQNKEE
B12	GlyR_A2	>sp|Q7TNC8|337-420	KEFLRLRRRQKRQNKEEDVT
B13	GlyR_A2	>sp|Q7TNC8|337-420	LRLRRRQKRQNKEEDVTRES
B14	GlyR_A2	>sp|Q7TNC8|337-420	RRRQKRQNKEEDVTRESRFN
B15	GlyR_A2	>sp|Q7TNC8|337-420	QKRQNKEEDVTRESRFNFSG
B16	GlyR_A2	>sp|Q7TNC8|337-420	QNKEEDVTRESRFNFSGYGM
B17	GlyR_A2	>sp|Q7TNC8|337-420	EEDVTRESRFNFSGYGMGHC
B18	GlyR_A2	>sp|Q7TNC8|337-420	VTRESRFNFSGYGMGHCLQM
B19	GlyR_A2	>sp|Q7TNC8|337-420	ESRFNFSGYGMGHCLQMKDG
B20	GlyR_A2	>sp|Q7TNC8|337-420	FNFSGYGMGHCLQMKDGTAV
B21	GlyR_A2	>sp|Q7TNC8|337-420	SGYGMGHCLQMKDGTAVKAT
B22	GlyR_A2	>sp|Q7TNC8|337-420	GMGHCLQMKDGTAVKATPAN
B23	GlyR_A2	>sp|Q7TNC8|337-420	HCLQMKDGTAVKATPANPLP
B24	GlyR_A2	>sp|Q7TNC8|337-420	QMKDGTAVKATPANPLPQPP
C1	GlyR_A2	>sp|Q7TNC8|337-420	DGTAVKATPANPLPQPPKDA
C2	GlyR_A2	>sp|Q7TNC8|337-420	AVKATPANPLPQPPKDADAI
C3	GlyR_A2	>sp|Q7TNC8|337-420	ATPANPLPQPPKDADAIKKK
C4	GlyR_A2	>sp|Q7TNC8|337-420	ANPLPQPPKDADAIKKKFVD
C5	GlyR_A2	>sp|Q7TNC8|337-420	LPQPPKDADAIKKKFVDRAK
C6	GlyR_A2	>sp|Q7TNC8|337-420	PPKDADAIKKKFVDRAKRID
C7	GlyR_A2	>sp|Q7TNC8|337-420	DADAIKKKFVDRAKRIDT
C8	GlyR_A3	>sp|Q91XP5|336-430	AVNFVSRQHKELLRFRRKRK
C9	GlyR_A3	>sp|Q91XP5|336-430	FVSRQHKELLRFRRKRKNKT
C10	GlyR_A3	>sp|Q91XP5|336-430	RQHKELLRFRRKRKNKTEAF

C11	GlyR_A3	>sp|Q91XP5|336-430	KELLRFRRKRKNKTEAFALE
C12	GlyR_A3	>sp|Q91XP5|336-430	LRFRRKRKNKTEAFALEKFY
C13	GlyR_A3	>sp|Q91XP5|336-430	RRKRKNKTEAFALEKFYRFS
C14	GlyR_A3	>sp|Q91XP5|336-430	RKNKTEAFALEKFYRFSDTD
C15	GlyR_A3	>sp|Q91XP5|336-430	KTEAFALEKFYRFSDTDDEV
C16	GlyR_A3	>sp|Q91XP5|336-430	AFALEKFYRFSDTDDEVRES
C17	GlyR_A3	>sp|Q91XP5|336-430	LEKFYRFSDTDDEVRESRFS
C18	GlyR_A3	>sp|Q91XP5|336-430	FYRFSDTDDEVRESRFSFTA
C19	GlyR_A3	>sp|Q91XP5|336-430	FSDTDDEVRESRFSFTAYGM
C20	GlyR_A3	>sp|Q91XP5|336-430	TDDEVRESRFSFTAYGMGPC
C21	GlyR_A3	>sp|Q91XP5|336-430	EVRESRFSFTAYGMGPCLQA
C22	GlyR_A3	>sp|Q91XP5|336-430	ESRFSFTAYGMGPCLQAKDG
C23	GlyR_A3	>sp|Q91XP5|336-430	FSFTAYGMGPCLQAKDGVVP
C24	GlyR_A3	>sp|Q91XP5|336-430	TAYGMGPCLQAKDGVVPKGP
D1	GlyR_A3	>sp|Q91XP5|336-430	GMGPCLQAKDGVVPKGPNHA
D2	GlyR_A3	>sp|Q91XP5|336-430	PCLQAKDGVVPKGPNHAVQV
D3	GlyR_A3	>sp|Q91XP5|336-430	QAKDGVVPKGPNHAVQVMPK
D4	GlyR_A3	>sp|Q91XP5|336-430	DGVVPKGPNHAVQVMPKSPD
D5	GlyR_A3	>sp|Q91XP5|336-430	VPKGPNHAVQVMPKSPDEMR
D6	GlyR_A3	>sp|Q91XP5|336-430	GPNHAVQVMPKSPDEMRKVF
D7	GlyR_A3	>sp|Q91XP5|336-430	HAVQVMPKSPDEMRKVFIDR
D8	GlyR_A3	>sp|Q91XP5|336-430	QVMPKSPDEMRKVFIDRAKK
D9	GlyR_A3	>sp|Q91XP5|336-430	PKSPDEMRKVFIDRAKKIDT
D10	GlyR_A4	>sp|Q2TB05|337-423	AVNFVSRQHKEFMRLRRRQR
D11	GlyR_A4	>sp|Q2TB05|337-423	FVSRQHKEFMRLRRRQRRQR
D12	GlyR_A4	>sp|Q2TB05|337-423	RQHKEFMRLRRRQRRQRMEE
D13	GlyR_A4	>sp|Q2TB05|337-423	KEFMRLRRRQRRQRMEEDII
D14	GlyR_A4	>sp|Q2TB05|337-423	MRLRRRQRRQRMEEDIIRES
D15	GlyR_A4	>sp|Q2TB05|337-423	RRRQRRQRMEEDIIRESRFY
D16	GlyR_A4	>sp|Q2TB05|337-423	QRRQRMEEDIIRESRFYFRG
D17	GlyR_A4	>sp| Q2TB05|337-423	QRMEEDIIRESRFYFRGYGL
D18	GlyR_A4	>sp| Q2TB05|337-423	EEDIIRESRFYFRGYGLGHC
D19	GlyR_A4	>sp| Q2TB05|337-423	IIRESRFYFRGYGLGHCLQA
D20	GlyR_A4	>sp| Q2TB05|337-423	ESRFYFRGYGLGHCLQARDG
D21	GlyR_A4	>sp| Q2TB05|337-423	FYFRGYGLGHCLQARDGGPM
D22	GlyR_A4	>sp| Q2TB05|337-423	RGYGLGHCLQARDGGPMEGS
D23	GlyR_A4	>sp| Q2TB05|337-423	GLGHCLQARDGGPMEGSSIY
D24	GlyR_A4	>sp| Q2TB05|337-423	HCLQARDGGPMEGSSIYSPQ
E1	GlyR_A4	>sp| Q2TB05|337-423	QARDGGPMEGSSIYSPQPPT

E2	GlyR_A4	>sp| Q2TB05|337-423	DGGPMEGSSIYSPQPPTPLL
E3	GlyR_A4	>sp| Q2TB05|337-423	PMEGSSIYSPQPPTPLLKEG
E4	GlyR_A4	>sp| Q2TB05|337-423	GSSIYSPQPPTPLLKEGETM
E5	GlyR_A4	>sp| Q2TB05|337-423	IYSPQPPTPLLKEGETMRKL
E6	GlyR_A4	>sp| Q2TB05|337-423	PQPPTPLLKEGETMRKLYVD
E7	GlyR_A4	>sp| Q2TB05|337-423	PTPLLKEGETMRKLYVDRAK
E8	GlyR_A4	>sp| Q2TB05|337-423	LLKEGETMRKLYVDRAKRID
E9	GlyR_A4	>sp| Q2TB05|337-423	EGETMRKLYVDRAKRIDT
F23	GABA_A1	>sp|P62812|334-420	NYFTKRGYAWDGKSVVPEKP
F24	GABA_A1	>sp|P62812|334-420	TKRGYAWDGKSVVPEKPKKV
G1	GABA_A1	>sp|P62812|334-420	GYAWDGKSVVPEKPKKVKDP
G2	GABA_A1	>sp|P62812|334-420	WDGKSVVPEKPKKVKDPLIK
G3	GABA_A1	>sp|P62812|334-420	KSVVPEKPKKVKDPLIKKNN
G4	GABA_A1	>sp|P62812|334-420	VPEKPKKVKDPLIKKNNTYA
G5	GABA_A1	>sp|P62812|334-420	KPKKVKDPLIKKNNTYAPTA
G6	GABA_A1	>sp|P62812|334-420	KVKDPLIKKNNTYAPTATSY
G7	GABA_A1	>sp|P62812|334-420	DPLIKKNNTYAPTATSYTPN
G8	GABA_A1	>sp|P62812|334-420	IKKNNTYAPTATSYTPNLAR
G9	GABA_A1	>sp|P62812|334-420	NNTYAPTATSYTPNLARGDP
G10	GABA_A1	>sp|P62812|334-420	YAPTATSYTPNLARGDPGLA
G11	GABA_A1	>sp|P62812|334-420	TATSYTPNLARGDPGLATIA
G12	GABA_A1	>sp|P62812|334-420	SYTPNLARGDPGLATIAKSA
G13	GABA_A1	>sp|P62812|334-420	PNLARGDPGLATIAKSATIE
G14	GABA_A1	>sp|P62812|334-420	ARGDPGLATIAKSATIEPKE
G15	GABA_A1	>sp|P62812|334-420	DPGLATIAKSATIEPKEVKP
G16	GABA_A1	>sp|P62812|334-420	LATIAKSATIEPKEVKPETK
G17	GABA_A1	>sp|P62812|334-420	IAKSATIEPKEVKPETKPPE
G18	GABA_A1	>sp|P62812|334-420	SATIEPKEVKPETKPPEPKK
G19	GABA_A1	>sp|P62812|334-420	IEPKEVKPETKPPEPKKTFN
G20	GABA_A1	>sp|P62812|334-420	KEVKPETKPPEPKKTFNSVS
G21	GABA_A1	>sp|P62812|334-420	KPETKPPEPKKTFNSVSKID
G22	GABA_A1	>sp|P62812|334-420	TKPPEPKKTFNSVSKIDR
G23	GABA_A2	>sp|P26048|335-419	NYFTKRGWAWDGKSVVNDKK
G24	GABA_A2	>sp|P26048|335-419	TKRGWAWDGKSVVNDKKKEK
H1	GABA_A2	>sp|P26048|335-419	GWAWDGKSVVNDKKKEKGSV
H2	GABA_A2	>sp|P26048|335-419	WDGKSVVNDKKKEKGSVMIQ
H3	GABA_A2	>sp|P26048|335-419	KSVVNDKKKEKGSVMIQNNA
H4	GABA_A2	>sp|P26048|335-419	VNDKKKEKGSVMIQNNAYAV
H5	GABA_A2	>sp|P26048|335-419	KKKEKGSVMIQNNAYAVAVA

H6	GABA_A2	>sp|P26048|335-419	EKGSVMIQNNAYAVAVANYA
H7	GABA_A2	>sp|P26048|335-419	SVMIQNNAYAVAVANYAPNL
H8	GABA_A2	>sp|P26048|335-419	IQNNAYAVAVANYAPNLSKD
H9	GABA_A2	>sp|P26048|335-419	NAYAVAVANYAPNLSKDPVL
H10	GABA_A2	>sp|P26048|335-419	AVAVANYAPNLSKDPVLSTI
H11	GABA_A2	>sp|P26048|335-419	VANYAPNLSKDPVLSTISKS
H12	GABA_A2	>sp|P26048|335-419	YAPNLSKDPVLSTISKSATT
H13	GABA_A2	>sp|P26048|335-419	NLSKDPVLSTISKSATTPEP
H14	GABA_A2	>sp|P26048|335-419	KDPVLSTISKSATTPEPNKK
H15	GABA_A2	>sp|P26048|335-419	VLSTISKSATTPEPNKKPEN
H16	GABA_A2	>sp|P26048|335-419	TISKSATTPEPNKKPENKPA
H17	GABA_A2	>sp|P26048|335-419	KSATTPEPNKKPENKPAEAK
H18	GABA_A2	>sp|P26048|335-419	TTPEPNKKPENKPAEAKKTF
H19	GABA_A2	>sp|P26048|335-419	EPNKKPENKPAEAKKTFNSV
H20	GABA_A2	>sp|P26048|335-419	KKPENKPAEAKKTFNSVSKI
H21	GABA_A2	>sp|P26048|335-419	ENKPAEAKKTFNSVSKIDR
J1	GABA_A4	>sp|Q9D6F4|341-521	NYFTNIQMQKAKKKISKPPP
J2	GABA_A4	>sp|Q9D6F4|341-521	TNIQMQKAKKKISKPPPEVP
J3	GABA_A4	>sp|Q9D6F4|341-521	QMQKAKKKISKPPPEVPAAP
J4	GABA_A4	>sp|Q9D6F4|341-521	KAKKKISKPPPEVPAAPVLK
J5	GABA_A4	>sp|Q9D6F4|341-521	KKISKPPPEVPAAPVLKEKH
J6	GABA_A4	>sp|Q9D6F4|341-521	SKPPPEVPAAPVLKEKHTET
J7	GABA_A4	>sp|Q9D6F4|341-521	PPEVPAAPVLKEKHTETSLQ
J8	GABA_A4	>sp|Q9D6F4|341-521	VPAAPVLKEKHTETSLQNTH
J9	GABA_A4	>sp|Q9D6F4|341-521	APVLKEKHTETSLQNTHANL
J10	GABA_A4	>sp|Q9D6F4|341-521	LKEKHTETSLQNTHANLNMR
J11	GABA_A4	>sp|Q9D6F4|341-521	KHTETSLQNTHANLNMRKRT
J12	GABA_A4	>sp|Q9D6F4|341-521	ETSLQNTHANLNMRKRTNAL
J13	GABA_A4	>sp|Q9D6F4|341-521	LQNTHANLNMRKRTNALVHS
J14	GABA_A4	>sp|Q9D6F4|341-521	THANLNMRKRTNALVHSESD
J15	GABA_A4	>sp|Q9D6F4|341-521	NLNMRKRTNALVHSESDVKS
J16	GABA_A4	>sp|Q9D6F4|341-521	MRKRTNALVHSESDVKSRTE
J17	GABA_A4	>sp|Q9D6F4|341-521	RTNALVHSESDVKSRTEVGN
J18	GABA_A4	>sp|Q9D6F4|341-521	ALVHSESDVKSRTEVGNHSS
J19	GABA_A4	>sp|Q9D6F4|341-521	HSESDVKSRTEVGNHSSKTS
J20	GABA_A4	>sp|Q9D6F4|341-521	SDVKSRTEVGNHSSKTSAVQ
J21	GABA_A4	>sp|Q9D6F4|341-521	KSRTEVGNHSSKTSAVQESS
J22	GABA_A4	>sp|Q9D6F4|341-521	TEVGNHSSKTSAVQESSEAT
J23	GABA_A4	>sp|Q9D6F4|341-521	GNHSSKTSAVQESSEATPKA

J24	GABA_A4	>sp|Q9D6F4|341-521	SSKTSAVQESSEATPKAHLA
K1	GABA_A4	>sp|Q9D6F4|341-521	TSAVQESSEATPKAHLASSP
K2	GABA_A4	>sp|Q9D6F4|341-521	VQESSEATPKAHLASSPNPF
K3	GABA_A4	>sp|Q9D6F4|341-521	SSEATPKAHLASSPNPFSRA
K4	GABA_A4	>sp|Q9D6F4|341-521	ATPKAHLASSPNPFSRANAA
K5	GABA_A4	>sp|Q9D6F4|341-521	KAHLASSPNPFSRANAAETM
K6	GABA_A4	>sp|Q9D6F4|341-521	LASSPNPFSRANAAETMSAA
K7	GABA_A4	>sp|Q9D6F4|341-521	SPNPFSRANAAETMSAAARG
K8	GABA_A4	>sp|Q9D6F4|341-521	PFSRANAAETMSAAARGLSS
K9	GABA_A4	>sp|Q9D6F4|341-521	RANAAETMSAAARGLSSAAS
K10	GABA_A4	>sp|Q9D6F4|341-521	AAETMSAAARGLSSAASPSP
K11	GABA_A4	>sp|Q9D6F4|341-521	TMSAAARGLSSAASPSPHGT
K12	GABA_A4	>sp|Q9D6F4|341-521	AAARGLSSAASPSPHGTLRP
K13	GABA_A4	>sp|Q9D6F4|341-521	RGLSSAASPSPHGTLRPASL
K14	GABA_A4	>sp|Q9D6F4|341-521	SSAASPSPHGTLRPASLGSA
K15	GABA_A4	>sp|Q9D6F4|341-521	ASPSPHGTLRPASLGSASTR
K16	GABA_A4	>sp|Q9D6F4|341-521	SPHGTLRPASLGSASTRPAF
K17	GABA_A4	>sp|Q9D6F4|341-521	GTLRPASLGSASTRPAFGSR
K18	GABA_A4	>sp|Q9D6F4|341-521	RPASLGSASTRPAFGSRLGR
K19	GABA_A4	>sp|Q9D6F4|341-521	SLGSASTRPAFGSRLGRIKT
K20	GABA_A4	>sp|Q9D6F4|341-521	SASTRPAFGSRLGRIKTTVN
K21	GABA_A4	>sp|Q9D6F4|341-521	TRPAFGSRLGRIKTTVNTTG
K22	GABA_A4	>sp|Q9D6F4|341-521	AFGSRLGRIKTTVNTTGAAG
K23	GABA_A4	>sp|Q9D6F4|341-521	SRLGRIKTTVNTTGAAGNVS
K24	GABA_A4	>sp|Q9D6F4|341-521	GRIKTTVNTTGAAGNVSATP
L1	GABA_A4	>sp|Q9D6F4|341-521	KTTVNTTGAAGNVSATPPPP
L2	GABA_A4	>sp|Q9D6F4|341-521	VNTTGAAGNVSATPPPPAPP
L3	GABA_A4	>sp|Q9D6F4|341-521	TGAAGNVSATPPPPAPPPSG
L4	GABA_A4	>sp|Q9D6F4|341-521	AGNVSATPPPPAPPPSGSGT
L5	GABA_A4	>sp|Q9D6F4|341-521	VSATPPPPAPPPSGSGTSKI
L6	GABA_A4	>sp|Q9D6F4|341-521	TPPPPAPPPSGSGTSKIDKY
L7	GABA_A4	>sp|Q9D6F4|341-521	PPAPPPSGSGTSKIDKYAR
L8	GABA_A5	>sp|Q8BHJ7|342-417	NYFTKRGWAWDGKKALEAAK
L9	GABA_A5	>sp|Q8BHJ7|342-417	TKRGWAWDGKKALEAAKIKK
L10	GABA_A5	>sp|Q8BHJ7|342-417	GWAWDGKKALEAAKIKKKER
L11	GABA_A5	>sp|Q8BHJ7|342-417	WDGKKALEAAKIKKKERELI
L12	GABA_A5	>sp|Q8BHJ7|342-417	KKALEAAKIKKKERELILNK
L13	GABA_A5	>sp|Q8BHJ7|342-417	LEAAKIKKKERELILNKSTN
L14	GABA_A5	>sp|Q8BHJ7|342-417	AKIKKKERELILNKSTNAFT

L15	GABA_A5	>sp|Q8BHJ7|342-417	KKKERELILNKSTNAFTTGK
L16	GABA_A5	>sp|Q8BHJ7|342-417	ERELILNKSTNAFTTGKLTH
L17	GABA_A5	>sp|Q8BHJ7|342-417	LILNKSTNAFTTGKLTHPPN
L18	GABA_A5	>sp|Q8BHJ7|342-417	NKSTNAFTTGKLTHPPNIPK
L19	GABA_A5	>sp|Q8BHJ7|342-417	TNAFTTGKLTHPPNIPKEQP
L20	GABA_A5	>sp|Q8BHJ7|342-417	FTTGKLTHPPNIPKEQPPAG
L21	GABA_A5	>sp|Q8BHJ7|342-417	GKLTHPPNIPKEQPPAGTAN
L22	GABA_A5	>sp|Q8BHJ7|342-417	THPPNIPKEQPPAGTANAPT
L23	GABA_A5	>sp|Q8BHJ7|342-417	PNIPKEQPPAGTANAPTVSI
L24	GABA_A5	>sp|Q8BHJ7|342-417	PKEQPPAGTANAPTVSIKAS
M1	GABA_A5	>sp|Q8BHJ7|342-417	QPPAGTANAPTVSIKASEEK
M2	GABA_A5	>sp|Q8BHJ7|342-417	AGTANAPTVSIKASEEKTAE
M3	GABA_A5	>sp|Q8BHJ7|342-417	ANAPTVSIKASEEKTAESK
M4	GABA_A6	>sp|P16305|325-419	NYFTNLQSQKAERQAQTAAT
M5	GABA_A6	>sp|P16305|325-419	TNLQSQKAERQAQTAATPPV
M6	GABA_A6	>sp|P16305|325-419	QSQKAERQAQTAATPPVAKS
M7	GABA_A6	>sp|P16305|325-419	KAERQAQTAATPPVAKSKAS
M8	GABA_A6	>sp|P16305|325-419	RQAQTAATPPVAKSKASESL
M9	GABA_A6	>sp|P16305|325-419	QTAATPPVAKSKASESLQAE
M10	GABA_A6	>sp|P16305|325-419	ATPPVAKSKASESLQAEIVV
M11	GABA_A6	>sp|P16305|325-419	PVAKSKASESLQAEIVVHSD
M12	GABA_A6	>sp|P16305|325-419	KSKASESLQAEIVVHSDSKY
M13	GABA_A6	>sp|P16305|325-419	ASESLQAEIVVHSDSKYHLK
M14	GABA_A6	>sp|P16305|325-419	SLQAEIVVHSDSKYHLKKRI
M15	GABA_A6	>sp|P16305|325-419	AEIVVHSDSKYHLKKRISSL
M16	GABA_A6	>sp|P16305|325-419	VVHSDSKYHLKKRISSLTLP
M17	GABA_A6	>sp|P16305|325-419	SDSKYHLKKRISSLTLPIVP
M18	GABA_A6	>sp|P16305|325-419	KYHLKKRISSLTLPIVPSSE
M19	GABA_A6	>sp|P16305|325-419	LKKRISSLTLPIVPSSEASK
M20	GABA_A6	>sp|P16305|325-419	RISSLTLPIVPSSEASKALS
M21	GABA_A6	>sp|P16305|325-419	SLTLPIVPSSEASKALSRTP
M22	GABA_A6	>sp|P16305|325-419	LPIVPSSEASKALSRTPILK
M23	GABA_A6	>sp|P16305|325-419	VPSSEASKALSRTPILKSTP
M24	GABA_A6	>sp|P16305|325-419	SEASKALSRTPILKSTPVSP
N1	GABA_A6	>sp|P16305|325-419	SKALSRTPILKSTPVSPPLL
N2	GABA_A6	>sp|P16305|325-419	LSRTPILKSTPVSPPLLLPA
N3	GABA_A6	>sp|P16305|325-419	TPILKSTPVSPPLLLPATGG
N4	GABA_A6	>sp|P16305|325-419	LKSTPVSPPLLLPATGGTSK
N5	GABA_A6	>sp|P16305|325-419	TPVSPPLLLPATGGTSKIDQ

N6	GABA_G1	>sp|Q9R0Y8|355-444	HYFTSNNKGKTTRGRKLKNK
N7	GABA_G1	>sp|Q9R0Y8|355-444	TSNNKGKTTRGRKLKNKTSA
N8	GABA_G1	>sp|Q9R0Y8|355-444	NKGKTTRGRKLKNKTSASPG
N9	GABA_G1	>sp|Q9R0Y8|355-444	KTTRGRKLKNKTSASPGLHA
N10	GABA_G1	>sp|Q9R0Y8|355-444	RGRKLKNKTSASPGLHAGST
N11	GABA_G1	>sp|Q9R0Y8|355-444	KLKNKTSASPGLHAGSTLIP
N12	GABA_G1	>sp|Q9R0Y8|355-444	NKTSASPGLHAGSTLIPMNS
N13	GABA_G1	>sp|Q9R0Y8|355-444	SASPGLHAGSTLIPMNSISL
N14	GABA_G1	>sp|Q9R0Y8|355-444	PGLHAGSTLIPMNSISLPQG
N15	GABA_G1	>sp|Q9R0Y8|355-444	HAGSTLIPMNSISLPQGEDD
N16	GABA_G1	>sp|Q9R0Y8|355-444	STLIPMNSISLPQGEDDYGY
N17	GABA_G1	>sp|Q9R0Y8|355-444	IPMNSISLPQGEDDYGYQCL
N18	GABA_G1	>sp|Q9R0Y8|355-444	NSISLPQGEDDYGYQCLEGK
N19	GABA_G1	>sp|Q9R0Y8|355-444	SLPQGEDDYGYQCLEGKDCT
N20	GABA_G1	>sp|Q9R0Y8|355-444	QGEDDYGYQCLEGKDCTSFF
N21	GABA_G1	>sp|Q9R0Y8|355-444	DDYGYQCLEGKDCTSFFCCF
N22	GABA_G1	>sp|Q9R0Y8|355-444	GYQCLEGKDCTSFFCCFDDC
N23	GABA_G1	>sp|Q9R0Y8|355-444	CLEGKDCTSFFCCFDDCRTG
N24	GABA_G1	>sp|Q9R0Y8|355-444	GKDCTSFFCCFDDCRTGSWR
O1	GABA_G1	>sp|Q9R0Y8|355-444	CTSFFCCFDDCRTGSWREGR
O2	GABA_G1	>sp|Q9R0Y8|355-444	FFCCFDDCRTGSWREGRIHI
O3	GABA_G1	>sp|Q9R0Y8|355-444	CFDDCRTGSWREGRIHIRIA
O4	GABA_G1	>sp|Q9R0Y8|355-444	DCRTGSWREGRIHIRIAKID
O5	GABA_G1	>sp|Q9R0Y8|355-444	TGSWREGRIHIRIAKIDSYS
O6	GABA_G1	>sp|Q9R0Y8|355-444	WREGRIHIRIAKIDSYSR

Supplementary table 3. FPS library. Wild-type peptides (in bold) correspond to the gephyrin-binding sequence of GlyR α2 subunit.

Position	Pepide Identifier	Uniprot correspondence	Peptide Sequence
A1	GlyRα2_FP_001	>sp|Q7TNC8|370-376	ANFSGYG
A2	GlyRα2_FP_002	>sp|Q7TNC8|370-376	CNFSGYG
A3	GlyRα2_FP_003	>sp|Q7TNC8|370-376	DNFSGYG
A4	GlyRα2_FP_004	>sp|Q7TNC8|370-376	ENFSGYG
A5	GlyRα2_FP_005	>sp|Q7TNC8|370-376	**FNFSGYG**
A6	GlyRα2_FP_006	>sp|Q7TNC8|370-376	GNFSGYG
A7	GlyRα2_FP_007	>sp|Q7TNC8|370-376	HNFSGYG
A8	GlyRα2_FP_008	>sp|Q7TNC8|370-376	INFSGYG

A9	GlyRα2_FP_009	>sp|Q7TNC8|370-376	KNFSGYG
A10	GlyRα2_FP_010	>sp|Q7TNC8|370-376	LNFSGYG
A11	GlyRα2_FP_011	>sp|Q7TNC8|370-376	MNFSGYG
A12	GlyRα2_FP_012	>sp|Q7TNC8|370-376	NNFSGYG
A13	GlyRα2_FP_013	>sp|Q7TNC8|370-376	PNFSGYG
A14	GlyRα2_FP_014	>sp|Q7TNC8|370-376	QNFSGYG
A15	GlyRα2_FP_015	>sp|Q7TNC8|370-376	RNFSGYG
A16	GlyRα2_FP_016	>sp|Q7TNC8|370-376	SNFSGYG
A17	GlyRα2_FP_017	>sp|Q7TNC8|370-376	TNFSGYG
A18	GlyRα2_FP_018	>sp|Q7TNC8|370-376	VNFSGYG
A19	GlyRα2_FP_019	>sp|Q7TNC8|370-376	WNFSGYG
A20	GlyRα2_FP_020	>sp|Q7TNC8|370-376	YNFSGYG
A21	GlyRα2_FP_021	>sp|Q7TNC8|370-376	FAFSGYG
A22	GlyRα2_FP_022	>sp|Q7TNC8|370-376	FCFSGYG
A23	GlyRα2_FP_023	>sp|Q7TNC8|370-376	FDFSGYG
A24	GlyRα2_FP_024	>sp|Q7TNC8|370-376	FEFSGYG
B1	GlyRα2_FP_025	>sp|Q7TNC8|370-376	FFFSGYG
B2	GlyRα2_FP_026	>sp|Q7TNC8|370-376	FGFSGYG
B3	GlyRα2_FP_027	>sp|Q7TNC8|370-376	FHFSGYG
B4	GlyRα2_FP_028	>sp|Q7TNC8|370-376	FIFSGYG
B5	GlyRα2_FP_029	>sp|Q7TNC8|370-376	FKFSGYG
B6	GlyRα2_FP_030	>sp|Q7TNC8|370-376	FLFSGYG
B7	GlyRα2_FP_031	>sp|Q7TNC8|370-376	FMFSGYG
B8	GlyRα2_FP_032	>sp|Q7TNC8|370-376	**FNFSGYG**
B9	GlyRα2_FP_033	>sp|Q7TNC8|370-376	FPFSGYG
B10	GlyRα2_FP_034	>sp|Q7TNC8|370-376	FQFSGYG
B11	GlyRα2_FP_035	>sp|Q7TNC8|370-376	FRFSGYG
B12	GlyRα2_FP_036	>sp|Q7TNC8|370-376	FSFSGYG
B13	GlyRα2_FP_037	>sp|Q7TNC8|370-376	FTFSGYG
B14	GlyRα2_FP_038	>sp|Q7TNC8|370-376	FVFSGYG
B15	GlyRα2_FP_039	>sp|Q7TNC8|370-376	FWFSGYG
B16	GlyRα2_FP_040	>sp|Q7TNC8|370-376	FYFSGYG
B17	GlyRα2_FP_041	>sp|Q7TNC8|370-376	FNASGYG
B18	GlyRα2_FP_042	>sp|Q7TNC8|370-376	FNCSGYG
B19	GlyRα2_FP_043	>sp|Q7TNC8|370-376	FNDSGYG
B20	GlyRα2_FP_044	>sp|Q7TNC8|370-376	FNESGYG
B21	GlyRα2_FP_045	>sp|Q7TNC8|370-376	**FNFSGYG**
B22	GlyRα2_FP_046	>sp|Q7TNC8|370-376	FNGSGYG
B23	GlyRα2_FP_047	>sp|Q7TNC8|370-376	FNHSGYG

B24	GlyRα2_FP_048	>sp|Q7TNC8|370-376	FNISGYG
C1	GlyRα2_FP_049	>sp|Q7TNC8|370-376	FNKSGYG
C2	GlyRα2_FP_050	>sp|Q7TNC8|370-376	FNLSGYG
C3	GlyRα2_FP_051	>sp|Q7TNC8|370-376	FNMSGYG
C4	GlyRα2_FP_052	>sp|Q7TNC8|370-376	FNNSGYG
C5	GlyRα2_FP_053	>sp|Q7TNC8|370-376	FNPSGYG
C6	GlyRα2_FP_054	>sp|Q7TNC8|370-376	FNQSGYG
C7	GlyRα2_FP_055	>sp|Q7TNC8|370-376	FNRSGYG
C8	GlyRα2_FP_056	>sp|Q7TNC8|370-376	FNSSGYG
C9	GlyRα2_FP_057	>sp|Q7TNC8|370-376	FNTSGYG
C10	GlyRα2_FP_058	>sp|Q7TNC8|370-376	FNVSGYG
C11	GlyRα2_FP_059	>sp|Q7TNC8|370-376	FNWSGYG
C12	GlyRα2_FP_060	>sp|Q7TNC8|370-376	FNYSGYG
C13	GlyRα2_FP_061	>sp|Q7TNC8|370-376	FNFAGYG
C14	GlyRα2_FP_062	>sp|Q7TNC8|370-376	FNFCGYG
C15	GlyRα2_FP_063	>sp|Q7TNC8|370-376	FNFDGYG
C16	GlyRα2_FP_064	>sp|Q7TNC8|370-376	FNFEGYG
C17	GlyRα2_FP_065	>sp|Q7TNC8|370-376	FNFFGYG
C18	GlyRα2_FP_066	>sp|Q7TNC8|370-376	FNFGGYG
C19	GlyRα2_FP_067	>sp|Q7TNC8|370-376	FNFHGYG
C20	GlyRα2_FP_068	>sp|Q7TNC8|370-376	FNFIGYG
C21	GlyRα2_FP_069	>sp|Q7TNC8|370-376	FNFKGYG
C22	GlyRα2_FP_070	>sp|Q7TNC8|370-376	FNFLGYG
C23	GlyRα2_FP_071	>sp|Q7TNC8|370-376	FNFMGYG
C24	GlyRα2_FP_072	>sp|Q7TNC8|370-376	FNFNGYG
D1	GlyRα2_FP_073	>sp|Q7TNC8|370-376	FNFPGYG
D2	GlyRα2_FP_074	>sp|Q7TNC8|370-376	FNFQGYG
D3	GlyRα2_FP_075	>sp|Q7TNC8|370-376	FNFRGYG
D4	GlyRα2_FP_076	>sp|Q7TNC8|370-376	**FNFSGYG**
D5	GlyRα2_FP_077	>sp|Q7TNC8|370-376	FNFTGYG
D6	GlyRα2_FP_078	>sp|Q7TNC8|370-376	FNFVGYG
D7	GlyRα2_FP_079	>sp|Q7TNC8|370-376	FNFWGYG
D8	GlyRα2_FP_080	>sp|Q7TNC8|370-376	FNFYGYG
D9	GlyRα2_FP_081	>sp|Q7TNC8|370-376	FNFSAYG
D10	GlyRα2_FP_082	>sp|Q7TNC8|370-376	FNFSCYG
D11	GlyRα2_FP_083	>sp|Q7TNC8|370-376	FNFSDYG
D12	GlyRα2_FP_084	>sp|Q7TNC8|370-376	FNFSEYG
D13	GlyRα2_FP_085	>sp|Q7TNC8|370-376	FNFSFYG
D14	GlyRα2_FP_086	>sp|Q7TNC8|370-376	**FNFSGYG**

D15	GlyRα2_FP_087	>sp|Q7TNC8|370-376	FNFSHYG
D16	GlyRα2_FP_088	>sp|Q7TNC8|370-376	FNFSIYG
D17	GlyRα2_FP_089	>sp|Q7TNC8|370-376	FNFSKYG
D18	GlyRα2_FP_090	>sp|Q7TNC8|370-376	FNFSLYG
D19	GlyRα2_FP_091	>sp|Q7TNC8|370-376	FNFSMYG
D20	GlyRα2_FP_092	>sp|Q7TNC8|370-376	FNFSNYG
D21	GlyRα2_FP_093	>sp|Q7TNC8|370-376	FNFSPYG
D22	GlyRα2_FP_094	>sp|Q7TNC8|370-376	FNFSQYG
D23	GlyRα2_FP_095	>sp|Q7TNC8|370-376	FNFSRYG
D24	GlyRα2_FP_096	>sp|Q7TNC8|370-376	FNFSSYG
E1	GlyRα2_FP_097	>sp|Q7TNC8|370-376	FNFSTYG
E2	GlyRα2_FP_098	>sp|Q7TNC8|370-376	FNFSVYG
E3	GlyRα2_FP_099	>sp|Q7TNC8|370-376	FNFSWYG
E4	GlyRα2_FP_100	>sp|Q7TNC8|370-376	FNFSYYG
E5	GlyRα2_FP_101	>sp|Q7TNC8|370-376	FNFSGAG
E6	GlyRα2_FP_102	>sp|Q7TNC8|370-376	FNFSGCG
E7	GlyRα2_FP_103	>sp|Q7TNC8|370-376	FNFSGDG
E8	GlyRα2_FP_104	>sp|Q7TNC8|370-376	FNFSGEG
E9	GlyRα2_FP_105	>sp|Q7TNC8|370-376	FNFSGFG
E10	GlyRα2_FP_106	>sp|Q7TNC8|370-376	FNFSGGG
E11	GlyRα2_FP_107	>sp|Q7TNC8|370-376	FNFSGHG
E12	GlyRα2_FP_108	>sp|Q7TNC8|370-376	FNFSGIG
E13	GlyRα2_FP_109	>sp|Q7TNC8|370-376	FNFSGKG
E14	GlyRα2_FP_110	>sp|Q7TNC8|370-376	FNFSGLG
E15	GlyRα2_FP_111	>sp|Q7TNC8|370-376	FNFSGMG
E16	GlyRα2_FP_112	>sp|Q7TNC8|370-376	FNFSGNG
E17	GlyRα2_FP_113	>sp|Q7TNC8|370-376	FNFSGPG
E18	GlyRα2_FP_114	>sp|Q7TNC8|370-376	FNFSGQG
E19	GlyRα2_FP_115	>sp|Q7TNC8|370-376	FNFSGRG
E20	GlyRα2_FP_116	>sp|Q7TNC8|370-376	FNFSGSG
E21	GlyRα2_FP_117	>sp|Q7TNC8|370-376	FNFSGTG
E22	GlyRα2_FP_118	>sp|Q7TNC8|370-376	FNFSGVG
E23	GlyRα2_FP_119	>sp|Q7TNC8|370-376	FNFSGWG
E24	GlyRα2_FP_120	>sp|Q7TNC8|370-376	**FNFSGYG**
F1	GlyRα2_FP_121	>sp|Q7TNC8|370-376	FNFSGYA
F2	GlyRα2_FP_122	>sp|Q7TNC8|370-376	FNFSGYC
F3	GlyRα2_FP_123	>sp|Q7TNC8|370-376	FNFSGYD
F4	GlyRα2_FP_124	>sp|Q7TNC8|370-376	FNFSGYE
F5	GlyRα2_FP_125	>sp|Q7TNC8|370-376	FNFSGYF

F6	GlyRα2_FP_126	>sp|Q7TNC8|370-376	**FNFSGYG**
F7	GlyRα2_FP_127	>sp|Q7TNC8|370-376	FNFSGYH
F8	GlyRα2_FP_128	>sp|Q7TNC8|370-376	FNFSGYI
F9	GlyRα2_FP_129	>sp|Q7TNC8|370-376	FNFSGYK
F10	GlyRα2_FP_130	>sp|Q7TNC8|370-376	FNFSGYL
F11	GlyRα2_FP_131	>sp|Q7TNC8|370-376	FNFSGYM
F12	GlyRα2_FP_132	>sp|Q7TNC8|370-376	FNFSGYN
F13	GlyRα2_FP_133	>sp|Q7TNC8|370-376	FNFSGYP
F14	GlyRα2_FP_134	>sp|Q7TNC8|370-376	FNFSGYQ
F15	GlyRα2_FP_135	>sp|Q7TNC8|370-376	FNFSGYR
F16	GlyRα2_FP_136	>sp|Q7TNC8|370-376	FNFSGYS
F17	GlyRα2_FP_137	>sp|Q7TNC8|370-376	FNFSGYT
F18	GlyRα2_FP_138	>sp|Q7TNC8|370-376	FNFSGYV
F19	GlyRα2_FP_139	>sp|Q7TNC8|370-376	FNFSGYW
F20	GlyRα2_FP_140	>sp|Q7TNC8|370-376	FNFSGYY
G1	GlyRα2_FP_PEG_001	>sp|Q7TNC8|370-376	ANFSGYGOO
G2	GlyRα2_FP_PEG_002	>sp|Q7TNC8|370-376	CNFSGYGOO
G3	GlyRα2_FP_PEG_003	>sp|Q7TNC8|370-376	DNFSGYGOO
G4	GlyRα2_FP_PEG_004	>sp|Q7TNC8|370-376	ENFSGYGOO
G5	GlyRα2_FP_PEG_005	>sp|Q7TNC8|370-376	**FNFSGYGOO**
G6	GlyRα2_FP_PEG_006	>sp|Q7TNC8|370-376	GNFSGYGOO
G7	GlyRα2_FP_PEG_007	>sp|Q7TNC8|370-376	HNFSGYGOO
G8	GlyRα2_FP_PEG_008	>sp|Q7TNC8|370-376	INFSGYGOO
G9	GlyRα2_FP_PEG_009	>sp|Q7TNC8|370-376	KNFSGYGOO
G10	GlyRα2_FP_PEG_010	>sp|Q7TNC8|370-376	LNFSGYGOO
G11	GlyRα2_FP_PEG_011	>sp|Q7TNC8|370-376	MNFSGYGOO
G12	GlyRα2_FP_PEG_012	>sp|Q7TNC8|370-376	NNFSGYGOO
G13	GlyRα2_FP_PEG_013	>sp|Q7TNC8|370-376	PNFSGYGOO
G14	GlyRα2_FP_PEG_014	>sp|Q7TNC8|370-376	QNFSGYGOO
G15	GlyRα2_FP_PEG_015	>sp|Q7TNC8|370-376	RNFSGYGOO
G16	GlyRα2_FP_PEG_016	>sp|Q7TNC8|370-376	SNFSGYGOO
G17	GlyRα2_FP_PEG_017	>sp|Q7TNC8|370-376	TNFSGYGOO
G18	GlyRα2_FP_PEG_018	>sp|Q7TNC8|370-376	VNFSGYGOO
G19	GlyRα2_FP_PEG_019	>sp|Q7TNC8|370-376	WNFSGYGOO
G20	GlyRα2_FP_PEG_020	>sp|Q7TNC8|370-376	YNFSGYGOO
G21	GlyRα2_FP_PEG_021	>sp|Q7TNC8|370-376	FAFSGYGOO
G22	GlyRα2_FP_PEG_022	>sp|Q7TNC8|370-376	FCFSGYGOO
G23	GlyRα2_FP_PEG_023	>sp|Q7TNC8|370-376	FDFSGYGOO
G24	GlyRα2_FP_PEG_024	>sp|Q7TNC8|370-376	FEFSGYGOO

H1	GlyRα2_FP_PEG_025	>sp|Q7TNC8|370-376	FFFSGYGOO
H2	GlyRα2_FP_PEG_026	>sp|Q7TNC8|370-376	FGFSGYGOO
H3	GlyRα2_FP_PEG_027	>sp|Q7TNC8|370-376	FHFSGYGOO
H4	GlyRα2_FP_PEG_028	>sp|Q7TNC8|370-376	FIFSGYGOO
H5	GlyRα2_FP_PEG_029	>sp|Q7TNC8|370-376	FKFSGYGOO
H6	GlyRα2_FP_PEG_030	>sp|Q7TNC8|370-376	FLFSGYGOO
H7	GlyRα2_FP_PEG_031	>sp|Q7TNC8|370-376	FMFSGYGOO
H8	GlyRα2_FP_PEG_032	>sp|Q7TNC8|370-376	**FNFSGYGOO**
H9	GlyRα2_FP_PEG_033	>sp|Q7TNC8|370-376	FPFSGYGOO
H10	GlyRα2_FP_PEG_034	>sp|Q7TNC8|370-376	FQFSGYGOO
H11	GlyRα2_FP_PEG_035	>sp|Q7TNC8|370-376	FRFSGYGOO
H12	GlyRα2_FP_PEG_036	>sp|Q7TNC8|370-376	FSFSGYGOO
H13	GlyRα2_FP_PEG_037	>sp|Q7TNC8|370-376	FTFSGYGOO
H14	GlyRα2_FP_PEG_038	>sp|Q7TNC8|370-376	FVFSGYGOO
H15	GlyRα2_FP_PEG_039	>sp|Q7TNC8|370-376	FWFSGYGOO
H16	GlyRα2_FP_PEG_040	>sp|Q7TNC8|370-376	FYFSGYGOO
H17	GlyRα2_FP_PEG_041	>sp|Q7TNC8|370-376	FNASGYGOO
H18	GlyRα2_FP_PEG_042	>sp|Q7TNC8|370-376	FNCSGYGOO
H19	GlyRα2_FP_PEG_043	>sp|Q7TNC8|370-376	FNDSGYGOO
H20	GlyRα2_FP_PEG_044	>sp|Q7TNC8|370-376	FNESGYGOO
H21	GlyRα2_FP_PEG_045	>sp|Q7TNC8|370-376	**FNFSGYGOO**
H22	GlyRα2_FP_PEG_046	>sp|Q7TNC8|370-376	FNGSGYGOO
H23	GlyRα2_FP_PEG_047	>sp|Q7TNC8|370-376	FNHSGYGOO
H24	GlyRα2_FP_PEG_048	>sp|Q7TNC8|370-376	FNISGYGOO
I1	GlyRα2_FP_PEG_049	>sp|Q7TNC8|370-376	FNKSGYGOO
I2	GlyRα2_FP_PEG_050	>sp|Q7TNC8|370-376	FNLSGYGOO
I3	GlyRα2_FP_PEG_051	>sp|Q7TNC8|370-376	FNMSGYGOO
I4	GlyRα2_FP_PEG_052	>sp|Q7TNC8|370-376	FNNSGYGOO
I5	GlyRα2_FP_PEG_053	>sp|Q7TNC8|370-376	FNPSGYGOO
I6	GlyRα2_FP_PEG_054	>sp|Q7TNC8|370-376	FNQSGYGOO
I7	GlyRα2_FP_PEG_055	>sp|Q7TNC8|370-376	FNRSGYGOO
I8	GlyRα2_FP_PEG_056	>sp|Q7TNC8|370-376	FNSSGYGOO
I9	GlyRα2_FP_PEG_057	>sp|Q7TNC8|370-376	FNTSGYGOO
I10	GlyRα2_FP_PEG_058	>sp|Q7TNC8|370-376	FNVSGYGOO
I11	GlyRα2_FP_PEG_059	>sp|Q7TNC8|370-376	FNWSGYGOO
I12	GlyRα2_FP_PEG_060	>sp|Q7TNC8|370-376	FNYSGYGOO
I13	GlyRα2_FP_PEG_061	>sp|Q7TNC8|370-376	FNFAGYGOO
I14	GlyRα2_FP_PEG_062	>sp|Q7TNC8|370-376	FNFCGYGOO
I15	GlyRα2_FP_PEG_063	>sp|Q7TNC8|370-376	FNFDGYGOO

I16	GlyRα2_FP_PEG_064	>sp|Q7TNC8|370-376	FNFEGYGOO
I17	GlyRα2_FP_PEG_065	>sp|Q7TNC8|370-376	FNFFGYGOO
I18	GlyRα2_FP_PEG_066	>sp|Q7TNC8|370-376	FNFGGYGOO
I19	GlyRα2_FP_PEG_067	>sp|Q7TNC8|370-376	FNFHGYGOO
I20	GlyRα2_FP_PEG_068	>sp|Q7TNC8|370-376	FNFIGYGOO
I21	GlyRα2_FP_PEG_069	>sp|Q7TNC8|370-376	FNFKGYGOO
I22	GlyRα2_FP_PEG_070	>sp|Q7TNC8|370-376	FNFLGYGOO
I23	GlyRα2_FP_PEG_071	>sp|Q7TNC8|370-376	FNFMGYGOO
I24	GlyRα2_FP_PEG_072	>sp|Q7TNC8|370-376	FNFNGYGOO
J1	GlyRα2_FP_PEG_073	>sp|Q7TNC8|370-376	FNFPGYGOO
J2	GlyRα2_FP_PEG_074	>sp|Q7TNC8|370-376	FNFQGYGOO
J3	GlyRα2_FP_PEG_075	>sp|Q7TNC8|370-376	FNFRGYGOO
J4	GlyRα2_FP_PEG_076	>sp|Q7TNC8|370-376	**FNFSGYGOO**
J5	GlyRα2_FP_PEG_077	>sp|Q7TNC8|370-376	FNFTGYGOO
J6	GlyRα2_FP_PEG_078	>sp|Q7TNC8|370-376	FNFVGYGOO
J7	GlyRα2_FP_PEG_079	>sp|Q7TNC8|370-376	FNFWGYGOO
J8	GlyRα2_FP_PEG_080	>sp|Q7TNC8|370-376	FNFYGYGOO
J9	GlyRα2_FP_PEG_081	>sp|Q7TNC8|370-376	FNFSAYGOO
J10	GlyRα2_FP_PEG_082	>sp|Q7TNC8|370-376	FNFSCYGOO
J11	GlyRα2_FP_PEG_083	>sp|Q7TNC8|370-376	FNFSDYGOO
J12	GlyRα2_FP_PEG_084	>sp|Q7TNC8|370-376	FNFSEYGOO
J13	GlyRα2_FP_PEG_085	>sp|Q7TNC8|370-376	FNFSFYGOO
J14	GlyRα2_FP_PEG_086	>sp|Q7TNC8|370-376	**FNFSGYGOO**
J15	GlyRα2_FP_PEG_087	>sp|Q7TNC8|370-376	FNFSHYGOO
J16	GlyRα2_FP_PEG_088	>sp|Q7TNC8|370-376	FNFSIYGOO
J17	GlyRα2_FP_PEG_089	>sp|Q7TNC8|370-376	FNFSKYGOO
J18	GlyRα2_FP_PEG_090	>sp|Q7TNC8|370-376	FNFSLYGOO
J19	GlyRα2_FP_PEG_091	>sp|Q7TNC8|370-376	FNFSMYGOO
J20	GlyRα2_FP_PEG_092	>sp|Q7TNC8|370-376	FNFSNYGOO
J21	GlyRα2_FP_PEG_093	>sp|Q7TNC8|370-376	FNFSPYGOO
J22	GlyRα2_FP_PEG_094	>sp|Q7TNC8|370-376	FNFSQYGOO
J23	GlyRα2_FP_PEG_095	>sp|Q7TNC8|370-376	FNFSRYGOO
J24	GlyRα2_FP_PEG_096	>sp|Q7TNC8|370-376	FNFSSYGOO
K1	GlyRα2_FP_PEG_097	>sp|Q7TNC8|370-376	FNFSTYGOO
K2	GlyRα2_FP_PEG_098	>sp|Q7TNC8|370-376	FNFSVYGOO
K3	GlyRα2_FP_PEG_099	>sp|Q7TNC8|370-376	FNFSWYGOO
K4	GlyRα2_FP_PEG_100	>sp|Q7TNC8|370-376	FNFSYYGOO
K5	GlyRα2_FP_PEG_101	>sp|Q7TNC8|370-376	FNFSGAGOO
K6	GlyRα2_FP_PEG_102	>sp|Q7TNC8|370-376	FNFSGCGOO

K7	GlyRα2_FP_PEG_103	>sp|Q7TNC8|370-376	FNFSGDGOO
K8	GlyRα2_FP_PEG_104	>sp|Q7TNC8|370-376	FNFSGEGOO
K9	GlyRα2_FP_PEG_105	>sp|Q7TNC8|370-376	FNFSGFGOO
K10	GlyRα2_FP_PEG_106	>sp|Q7TNC8|370-376	FNFSGGGOO
K11	GlyRα2_FP_PEG_107	>sp|Q7TNC8|370-376	FNFSGHGOO
K12	GlyRα2_FP_PEG_108	>sp|Q7TNC8|370-376	FNFSGIGOO
K13	GlyRα2_FP_PEG_109	>sp|Q7TNC8|370-376	FNFSGKGOO
K14	GlyRα2_FP_PEG_110	>sp|Q7TNC8|370-376	FNFSGLGOO
K15	GlyRα2_FP_PEG_111	>sp|Q7TNC8|370-376	FNFSGMGOO
K16	GlyRα2_FP_PEG_112	>sp|Q7TNC8|370-376	FNFSGNGOO
K17	GlyRα2_FP_PEG_113	>sp|Q7TNC8|370-376	FNFSGPGOO
K18	GlyRα2_FP_PEG_114	>sp|Q7TNC8|370-376	FNFSGQGOO
K19	GlyRα2_FP_PEG_115	>sp|Q7TNC8|370-376	FNFSGRGOO
K20	GlyRα2_FP_PEG_116	>sp|Q7TNC8|370-376	FNFSGSGOO
K21	GlyRα2_FP_PEG_117	>sp|Q7TNC8|370-376	FNFSGTGOO
K22	GlyRα2_FP_PEG_118	>sp|Q7TNC8|370-376	FNFSGVGOO
K23	GlyRα2_FP_PEG_119	>sp|Q7TNC8|370-376	FNFSGWGOO
K24	GlyRα2_FP_PEG_120	>sp|Q7TNC8|370-376	**FNFSGYGOO**
L1	GlyRα2_FP_PEG_121	>sp|Q7TNC8|370-376	FNFSGYAOO
L2	GlyRα2_FP_PEG_122	>sp|Q7TNC8|370-376	FNFSGYCOO
L3	GlyRα2_FP_PEG_123	>sp|Q7TNC8|370-376	FNFSGYDOO
L4	GlyRα2_FP_PEG_124	>sp|Q7TNC8|370-376	FNFSGYEOO
L5	GlyRα2_FP_PEG_125	>sp|Q7TNC8|370-376	FNFSGYFOO
L6	GlyRα2_FP_PEG_126	>sp|Q7TNC8|370-376	**FNFSGYGOO**
L7	GlyRα2_FP_PEG_127	>sp|Q7TNC8|370-376	FNFSGYHOO
L8	GlyRα2_FP_PEG_128	>sp|Q7TNC8|370-376	FNFSGYIOO
L9	GlyRα2_FP_PEG_129	>sp|Q7TNC8|370-376	FNFSGYKOO
L10	GlyRα2_FP_PEG_130	>sp|Q7TNC8|370-376	FNFSGYLOO
L11	GlyRα2_FP_PEG_131	>sp|Q7TNC8|370-376	FNFSGYMOO
L12	GlyRα2_FP_PEG_132	>sp|Q7TNC8|370-376	FNFSGYNOO
L13	GlyRα2_FP_PEG_133	>sp|Q7TNC8|370-376	FNFSGYPOO
L14	GlyRα2_FP_PEG_134	>sp|Q7TNC8|370-376	FNFSGYQOO
L15	GlyRα2_FP_PEG_135	>sp|Q7TNC8|370-376	FNFSGYROO
L16	GlyRα2_FP_PEG_136	>sp|Q7TNC8|370-376	FNFSGYSOO
L17	GlyRα2_FP_PEG_137	>sp|Q7TNC8|370-376	FNFSGYTOO
L18	GlyRα2_FP_PEG_138	>sp|Q7TNC8|370-376	FNFSGYVOO
L19	GlyRα2_FP_PEG_139	>sp|Q7TNC8|370-376	FNFSGYWOO
L20	GlyRα2_FP_PEG_140	>sp|Q7TNC8|370-376	FNFSGYYOO